



**EFFECTS OF THERMAL TREATMENT ON MECHANICAL AND  
MORPHOLOGICAL PROPERTIES OF ALUMINIUM ALLOY REINFORCED  
WITH CHITOSAN**

**BY**

**EZEKIEL VICTOR UCHECHUKWU  
16CD021596**

**BEING A FINAL YEAR REPORT SUBMITTED TO  
THE DEPARTMENT OF MECHANICAL ENGINEERING,  
COLLEGE OF ENGINEERING,  
COVENANT UNIVERSITY, OTA, OGUN STATE, NIGERIA**

**IN PARTIAL FULFILMENT  
OF THE REQUIREMENTS FOR THE AWARD OF  
BACHELOR OF ENGINEERING DEGREE B.Eng. (Hons.)  
IN  
MECHANICAL ENGINEERING**

**OCTOBER, 2021**

## **DECLARATION**

I humbly declare that the work detailed in this project titled, “EFFECTS OF THERMAL TREATMENT ON MECHANICAL AND MORPHOLOGICAL PROPERTIES OF ALUMINIUM ALLOY REINFORCED WITH CHITOSAN” was carried out by me under the supervision of Dr. Udoye N. Ekene in the Department of Mechanical Engineering, Covenant University. Also, I attest to the best of my knowledge that this report has not been submitted here or elsewhere in a previous application for a bachelor’s degree award. All sources of knowledge used have been duly acknowledged.

.....

Ezekiel Victor Uchechukwu

16CD021596

## **CERTIFICATION**

This is to certify that I, EZEKIEL VICTOR UCHECHUKWU carried out this research project under my supervisor in the Department of Mechanical Engineering, Covenant University, Ota.

---

Dr. Nduka Ekene Udoye

Date

Supervisor

---

Professor Joshua Olusegun Okeniyi

Date

Head of Department

## **DEDICATION**

This research project is dedicated to God for His Grace accorded to me to carry out this project.

## **ACKNOWLEDGEMENT**

I am thankful to God Almighty for the enablement to complete this research work. I also wish to acknowledge my supervisor, Dr. Nduka Ekene Udoye for his dedication and assistance in seeing this through. I am indebted to my mother and sister for their constant prayers, love, support, and motivation not to give up.

## ABSTRACT

The immense cost and adverse environmental effect of producing aluminium matrix composites (AMC) manufactured conventionally compel replacement with eco-friendly material of enhanced mechanical, electrical and thermal properties. Repurposing agricultural waste in advanced materials plays an important role in driving a sustainable society. This study inspired by global sustainable development goals investigates the characteristic electro-thermo-mechano-morphological behaviours of AA6061/chitosan at sieve size of 90 $\mu$ m developed using modified stir casting at weight proportions: 3, 6, 9, 12wt.%. The hardness property of the fabricated samples were characterized by a Brinell hardness tester. While the ultimate tensile strength of the composites were observed on a TecQuipment universal testing machine (SM1000), the scanning electron micrograph (SEM) and energy dispersive spectroscopy (EDS) provide micro-structural imagery and elemental quantification, respectively. The phase composition of the developed samples is obtained using the X'pert powder x-ray diffractometer. Similarly, the ammeter-voltmeter technique is used to estimate the resistivity and conductivity of the casted samples. The thermal conductivity behaviour of the composites developed was evaluated using forced convection green-house using heat-transfer parameter measurements from anemometer, hygrometer, thermometer and solarimeter. The introduction of chitosan to the AA6061 matrix yielded an increase in the hardness property of the alloy. The hardness of the developed composites improved correspondingly with an increased weight proportion of reinforcement, attaining a maximum of 60.2 HRB at 9wt.% chitosan equivalent to 2.36% improvement in AA6061 hardness, 57.4 HRB. Likewise, tensile strength enhanced with increasing chitosan particulates from 83.07MPa recorded for the unreinforced alloy to a maximum of 114.92MPa for 12wt.% AA6061 reinforcement with chitosan. Furthermore, the microstructural of AA6061 with chitosan strains of Reinforcement was observed in the AA6061/3wt.% SEM eventually filling grain boundaries of the metal with increasing reinforcements to provide evenly distributed fibrous links connecting AA6061 grain structure at 6wt.% and 9wt.% reinforcement in the micrograph. The fibrous links provide load transfer observed in the improved tensile strength. Similarly, calcium and oxygen constituents grew in the composites with increasing reinforcements. The XRD of the samples showed concrete evidence of Hydroxyapatite,  $\text{Ca}_{10}(\text{PO}_4)_6(\text{OH})_2$ , a component of teeth and bones responsible for strength, justified by several high-intensity peaks of the dominant crystal in the diffractogram. Electrical conductivity improved for the increasing weight proportions of chitosan in fabricated samples to a maximum of 38.197186S/m in 12wt.% chitosan, from 37.81S/m of as-cast alloy. Conversely, 189.40W/mK represents the maximum thermal conductivity results of developed composites, AA 6061 + 9wt.% chitosan analysed by forced convection under greenhouse conditions. The thermal conductivity increased from 3wt.% to 9wt.% (124.16, 141.58, and 189.40 189.40W/mK), but notably declined to 141.58W/mK at 12wt.% of reinforcement. Still, the improvements failed to enhance the thermal conductivity coefficient of the alloy, recorded at 362.97W/mK. Thus, the addition of chitosan insulated and increased the thermal resistivity of the alloy. Based on the results, chitosan reinforced AMMC can be manufactured through the economic stir casting process yet satisfy design requirements to be applied in electrical cables due to its improved mechanical strength and electrical conductivity and lightweight household utensils due to antibacterial properties of chitosan.

## TABLE OF CONTENTS

1	INTRODUCTION.....	1
1.1	Background of the Study.....	1
1.2	Problem Statement .....	3
1.3	Research Aim And Objectives .....	3
1.3.1	Aim.....	3
1.3.2	Objectives.....	3
1.4	Justification of the Study.....	4
1.5	Scope and Limitation of the Study.....	4
1.6	Significance of the Study .....	4
2	LITERATURE REVIEW.....	5
2.1	Introduction .....	5
2.2	Types of Composites Materials.....	8
2.2.1	Advancement of composites .....	8
2.2.2	Metal matrix composites .....	9
2.2.3	Polymer matrix composites .....	9
2.2.4	Ceramic matrix composites.....	10
2.2.5	Applications of aluminium alloys .....	10
2.2.6	Marine sector.....	11
2.2.7	Automotive sector .....	11
2.2.8	Construction sector.....	11
2.2.9	Transportation sector.....	12
2.2.10	Electrical sector.....	12
2.2.11	Consumer goods.....	12
2.2.12	Advantages of aluminium alloys.....	12
2.2.13	Disadvantages of aluminium alloys .....	13
2.2.14	Review of aluminium alloy/synthetic ceramic composite .....	13
2.2.15	Review of aluminium alloy/biodegradable reinforced materials .....	16
2.2.16	Review of hybrid reinforcement on aluminium alloy .....	21
2.2.17	Review of chitosan as reinforcement .....	24
2.2.18	Review of thermal properties and effects of heat treatment of AMMC.....	25
2.3	Stir Casting.....	28
3	MATERIALS AND METHODOLOGY .....	31
3.1	Introduction .....	31
3.2	Materials.....	31
3.2.1	Workpiece .....	31

3.2.2	Reinforcement .....	32
3.2.3	Reinforcing technique .....	33
3.2.4	Scanning electron microscope (SEM)/ Energy dispersive spectroscopy (EDS).....	34
3.2.5	X-ray diffractometer (XRD).....	35
3.2.6	Micro-hardness tester .....	36
3.2.7	Tensile testing machine.....	37
3.2.8	Cutting machine .....	38
3.2.9	Electrical analytical weighing balance.....	39
3.2.10	Electrical properties testing.....	39
3.2.11	Thermal properties testing.....	40
3.3	Material And Methods .....	41
3.3.1	Sectioning.....	41
3.3.2	The proportion of reinforcing particulate.....	41
3.3.3	Preparation of reinforced aluminium composite.....	42
3.3.4	Characteristics of reinforced aluminium composite.....	42
3.3.5	X-ray diffractometer (XRD).....	42
3.3.6	Scanning electron microscope.....	43
3.3.7	Microhardness testing .....	43
3.3.8	Tensile testing .....	43
3.3.9	Electrical properties testing.....	44
3.3.10	Thermal properties testing.....	45
3.4	Conclusion.....	45
4	RESULTS AND DISCUSSIONS .....	46
4.1	Introduction .....	46
4.2	Aluminium Reinforcement With Chitosan .....	46
4.2.1	Microhardness analysis of chitosan reinforced aluminium alloy AA6061 .....	46
4.2.2	Ultimate tensile strength for chitosan reinforced AA6061 and unreinforced AA6061 .....	48
4.2.3	Scanning electron microscope and Energy disperse spectroscopy analyses.....	51
4.2.4	X-ray diffraction analysis of reinforced composites .....	56
4.2.5	Thermal properties: conductive heat transfer coefficient.....	60
4.2.6	Electrical properties: resistivity and conductivity.....	62
5	CONCLUSION AND RECOMMENDATIONS.....	65
5.1	Introduction .....	65
5.2	Conclusions .....	65
5.3	Final Conclusion .....	66
5.4	Recommendations .....	66

## TABLE OF TABLES

Table 3.1: Chemical Composition of AA6061 .....	32
Table 3.2: Mechanical Properties of AA6061 .....	32
Table 3.3: Physical Properties of AA6061 .....	32
Table 4.1: Reinforcement Weight Parameters.....	46
Table 4.2: Hardness test result of samples .....	47
Table 4.3: Showing the maximum stress of the control sample.....	48
Table 4.4: Showing Tensile Stress at Break of the unreinforced specimen .....	49
Table 4.5: Showing the maximum stress of the reinforced specimens .....	50
Table 4.6: Showing Tensile Stress at Break of the reinforced specimens.....	50
Table 4.7: Result of Heat Transfer Coefficient of Composite.....	62
Table 4.8: Result of Electrical Resistivity and Conductivity of Samples .....	63

## TABLE OF FIGURES

Figure 3.1: Dried Micropogonias undulatus scales .....	33
Figure 3.2: Stir casting furnace .....	34
Figure 3.3: Scanning Electron Microscope .....	35
Figure 3.4: X-Ray Diffractometer .....	36
Figure 3.5: Universal Testing Machine .....	38
Figure 3.6: Cutting Machine.....	38
Figure 3.7: OHAUS PioneerTM PA214 Model .....	39
Figure 3.8: Electrical properties testing experiment setup .....	40
Figure 3.9: Thermal properties testing experiment setup.....	41
Figure 3.10: Electrical properties testing experiment circuitry .....	44
Figure 4.1: Hardness test result of samples .....	48
Figure 4.2: Showing Tensile Strength of unreinforced AA6061 alloy .....	49
Figure 4.3: Showing Tensile Strength of the reinforced Al6061 alloy matrix composites....	51
Figure 4.4: (a) Micrograph of Control Sample AA6061. (b) Energy Dispersive Spectra Showing the Mineral Content of Control Sample AA6061 .....	52
Figure 4.5: (a) SEM image of AA6061+3wt. %Chitosan. (b) EDS of specimen.....	53
Figure 4.6: (a) SEM image of AA6061+ 6wt % Chitosan. (b) EDS of specimen.....	54
Figure 4.7: (a) SEM image of AA6061+ 9 wt. % Chitosan. (b) EDS of specimen.....	54
Figure 4.8: (a) SEM image of AA6061+ 12 wt. % Chitosan. (b) EDS of specimen.....	55
Figure 4.9: XRD Spectrum of pure As-received Aluminium Alloy .....	56
Figure 4.10: XRD of AA6061+3 wt.% Chitosan .....	57
Figure 4.11: XRD of AA6061+6wt% Chitosan .....	58
Figure 4.12: XRD of AA6061+9wt.% chitosan .....	58
Figure 4.13: XRD of AA6061+12wt% chitosan .....	59
Figure 4.14: Surface Convective Heat Transfer Coefficient .....	60
Figure 4.15: Surface Temperature of Composite .....	61
Figure 4.16: Error bars of Conductive Heat Transfer Coefficient of Samples.....	61
Figure 4.17: Effects of Chitosan on Resistivity of AA6061 .....	63
Figure 4.18: Effects of Chitosan on Conductivity of AA6061.....	64

# CHAPTER ONE

## 1 INTRODUCTION

### 1.1 Background of the Study

The selection of homogenous materials has come with trade-offs in strength and weight, limiting them from application in many industries. In such industries, these monolithic materials do not satisfy the material selection process, which aims at identifying materials that provide appropriate geometry and properties necessary for products at the lowest cost and maximum efficiency (Waterman, 1982). As a result, technological developments in material science show continued interest in achieving all the integral desired properties for applications. Hence, the departure in engineering applications from homogenous and monolithic material to new materials called composites (Sijo & Jayadevan, 2016).

Consequently, composites can be said to have added a stunning fluidity to design engineering, compelling scientists, and engineers to create a different material for each application as they pursue saving in weight and cost (Schier & Juergens, 1983). In simple terms, composite materials are a form of fusing homogenous or heterogenous materials. Composites range from embedding bulk matrix of a homogeneous or heterogeneous material with reinforcement phase to reinforcing homogeneous material by technically “glueing” materials together, with the first composites said to have been created by the Mesopotamians by glueing wooden strips at different angles to create plywood. A material matrix is a base homogeneous or monolithic material that lodges reinforcement fibres. The matrix provides a medium for binding and protection reinforcement material while the fibres receive loading and stresses.

Metal matrix composites (MMCs) are a group of materials (such as metals, alloys, or intermetallic compounds) incorporated with various reinforcing phases, such as particulates, whiskers, or continuous fibres. MMCs offer the benefit of obtaining a mix of desired properties, resulting in the strategic selection of metal matrixes and reinforcement. In the structural application, where the aim is to obtain lighter and stronger materials, the matrix comprises aluminium, magnesium, and titanium. In high-temperature applications, commonly used are cobalt and cobalt-nickel. However, it is worth noting that MMCs are expensive to develop (Li & Gao, 2008)

In industrial applications, metal matrix composites (MMCs) like the AA6000 series (AA6061/6063) are significant for lightweight materials with high specific strength, stiffness, and heat resistance. The casting procedure for processing MMCs is an auspicious means of producing complex form composites at a reasonable cost (Kulkarni et al., 2019).

Similarly, with research efforts geared towards curtailing environmental pollution and promoting eco-friendliness, agricultural and industrial waste products are now considered rich sources of reinforcement materials. These underutilized materials are for metal matrix composite providing similar properties as their synthetic counterparts without toxic residue produced due to manufacturing inorganic materials. Hence, a lasting solution to utilizing agro-waste for advanced material production is both of massive economic and environmental impact, since achieving optimal material selection while preferentially selecting renewable materials over non-renewable materials is one of the sustainability goals of the modern society. (Ermolaeva et al., 2002).

Hence, cost savings can be realized by the production of materials using agro-waste and other sustainable materials. The high cost of producing aluminium metal composite can see a massive decrease due to the use of readily available material as reinforcement fibre. This study aims to scale up the production processes, which will enable composites reinforced agro-wastes designed into different products with the maximum achievable properties (Abba et al., 2013; Kulkarni et al., 2019).

Typically, aluminium's recyclability, environmental friendliness, and low production cost qualify it for sustainable economic use. In particular, recycled aluminium contributes to the aluminium demand and take 5% of the production cost of virgin aluminium (Davis, 2001). Likewise, aluminium desirable mechanical, thermal and chemical properties have led to its continued utility in transportation, construction, manufacturing, and packaging. Also, aluminium provides a matrix for embedding materials like silicon carbide or continuous carbide to achieve light and strong structural aims.

Globally, industrial aquatic organism waste and discards from fishing continue to grow in hundreds of millions of tonnes every year. Although the waste is naturally disintegrating, the degradation happens slowly to the tremendous amount of waste consisting of tails, heads and internal organs (Gokulalakshmi et al., 2017; Zeller et al., 2018). These wastes contain valuable materials such as consistent chitosan, a biopolymer, which is responsible for strength in bones, teeth, and scales of crustaceans. Thus, this study was inspired by global sustainability goals to

utilize agricultural waste in the production of composite material. Using chitosan derived from *Micropogonias undulatus* scales as the reinforcement material in AA6061 alloy bulk matrix, the resulting material would be investigated strength, wear resistance, thermal resistance, and corrosion-resistant properties.

## 1.2 Problem Statement

Aluminium matrix composites provide more beneficial properties than monolithic aluminium metals and alloys. However, hybrid and composites are not used often due to factors affecting the economics of scale:

- Cost of reinforcement material
- Cost of production technique

Hence, considerations must be put into the development of composite, mainly the selection of material and techniques, to ensure that significant cost implications do not outweigh the benefits of improved properties. These issues are adequately addressed in this study.

## 1.3 Research Aim and Objectives

### 1.3.1 Aim

This research project aims to examine the potency of chitosan as a reinforcement material for aluminium alloy AA6061.

### 1.3.2 Objectives

1. To develop composite material using aluminium alloy composite of fish scale collagen, chitosan, as a reinforcement phase in AA6061 aluminium alloy composite matrix
2. To investigate the surface morphology of the composite via SEM (Scanning Electron Microscope)/ EDS (Energy Dispersive Spectroscopy) and X-ray Diffractometer for crystalline phase analysis.
3. To obtain the characterization of composite using mechanical testing: hardness, tensile and elongation properties.
4. To perform electrical properties test, conductivity, on the newly formed metal matrix composite.

## **1.4 Justification of the Study**

The reinforcement of aluminium alloy with chitosan lead to:

1. Enhanced mechanical and thermal properties of hybrid aluminium metal matrix composite (AMMC)
2. Safer and sustainable application of the agricultural waste product, chitosan.

## **1.5 Scope and Limitation of the Study**

The scope of the project is stated as follows:

1. Preparation of composite using the stir casting technique
2. Microstructural/morphological characterization of composite using (SEM / EDS, XRD)
3. Mechanical testing (hardness, elongation, and tensile stress) of prepared composites
4. Electrical test

The study is limited to reinforcement with chitosan derived from *Micropogonias undulatus* only.

## **1.6 Significance of the Study**

This research project addresses the topic of AA6061 aluminium hybrid matrix reinforcement with chitosan, providing data for selecting the new material with an emphasis on thermal behaviours.

## CHAPTER TWO

### 2 LITERATURE REVIEW

#### 2.1 Introduction

Design engineering requires the proper selection of materials, which provides adequate mechanical, thermal, and chemical behaviours required by part or component while satisfying cost and weight constraints. Hence, the importance of composites to provide a blend of properties from different homogeneous and heterogeneous constituting materials. The successful application of metal matrix composites has seen performance improvement in aerospace and automotive applications resulting in cost and weight savings and increased efficiency.

As noted by (Chawla, 2016), composite needs to satisfy the following conditions:

- It is fabricated (excludes natural composites such as wood).
- It is made of multiple physically and chemically distinct, appropriately dispersed phases separated by an interface.
- Its properties cannot be described singly by its components.

Aluminium and its alloys possess resistance to progressive oxidization, high formability, nonpyrophoric properties, high conductivity. Hence, they are the ideal raw material for products, from simple cooking utensils to advanced aircraft. To maintain a standard for categorizing aluminium and its alloys due to ubiquity, the aluminium association developed a classification system of aluminium and its alloys. This system classifies aluminium alloys in two significant categories wrought alloys and cast alloys compositions using nine series in each category to identify the alloys to make a differentiation between categories based on a property development mechanism to classify the alloys further. In this differentiation, four digits are used to distinguish individual series, where the first digit represents the dominant alloying constituent, while the second digit connotes alterations to the main alloy. The penultimate and final digits in a series (family) representation are randomly assigned to individual alloys in the series (Davis, 2001). Table 2.1 represents the aluminium association's system of classification of aluminium alloys.

**Table 2.1: Classification of Aluminium Alloys**

Wrought alloy	
<b>Series</b>	<b>Description</b>
1xxx	Control metal comprising of unalloyed (pure) aluminium used in the production of rotors.
2xxx	Copper is the primary alloying ingredient in these alloys with additional alloying components specified.
3xxx	Silicon as major alloying constituent of aluminium with other alloying elements: magnesium and copper. The series is used in 90 percent of all shape casted products.
4xxx	Alloys of aluminium with silicon as primary alloying constituent.
5xxx	Alloys of aluminium with magnesium as primary alloying element.
6xxx	Unused
7xxx	Alloys of aluminium with zinc as primary constituent with other composing elements such as copper and magnesium, specified.
8xxx	Alloys of aluminium with tin as primary alloying element.
9xxx	Not used
Heat-treatable	

Cast alloy

Wrought alloy	
<b>Series</b>	<b>Description</b>
1xxx	Controlled pure aluminium, referred to as control alloy, is majorly used in the chemical and electrical industry.
2xxx	Copper is the most common alloying element, while other elements, such as magnesium, can be selected. The high strength of 2xxx-series alloys (yield strengths as high as 455 MPa, or 66 ksi) makes them popular in aviation.

3xxx	Manganese-based alloys, which are utilized as general-purpose alloys for architectural purposes and a variety of items.
4xxx	Alloys containing silicon as the primary alloying element, which are utilized in welding rods and brazing sheets.
5xxx	Alloys with magnesium as the primary alloying element, which are utilized in boat hulls, gangplanks, and other marine-related products.
6xxx	Magnesium and silicon are the main alloying constituents in these alloys, which are extensively utilized in architectural extrusions and automotive components.
7xxx	Alloys in which zinc is the principal alloying element (although other elements, such as copper, magnesium, chromium, and zirconium, may be specified), used in aircraft structural components and other high-strength applications. The 7xxx series are the strongest aluminium alloys, with yield strengths $\geq 500$ MPa ( $\geq 73$ ksi) possible.
8xxx	Aluminium alloy with significant proportions of lithium, tin, or iron as constituent elements.
9xxx	This series has been set aside for future alloys.

---

In terms of structural response, research on aluminium alloys has concentrated chiefly on wrought alloys, notably the 5xxx and 6xxx series, which are the most appealing for structural engineering applications because of their mechanical characteristics (Georgantzia et al., 2021). In corrosive environments, such as sea water, aluminium-based alloys have often been applied. Hence a reinforcement of aluminium bulk matrix with substantial fortification particles while create longer-lasting composite material (Fayomi et al., 2019).

Composite material is a materials system composed of a suitably arranged mixture or combination of two or more constituents of differing structure in the macro and micro range such that each constituent in the resulting mixture are insoluble and possess a bounding interface between them (Smith et al., 2019). The resulting composite is characterized as a combination of its constituent material providing specific desirable properties compared to those of its segments (Sanusi et al., 2015).

## **2.2 Types of Composites Materials**

The word "composite" corresponds to a compound structure made up of separate elements (reinforcements) dispersed in a continuous or interminable manner (the matrix), with the properties of the newly formed compound derived from the properties of the individual constituents and the grain boundaries between different constituents. It is a mixture of two or more constituents that differ in physical and chemical characteristics from those of its components alone.

Composites are combinations of the primary classes of materials (metal–ceramic, metal–polymer, or polymer–ceramic). The composite materials are broadly classified into two categories based on the matrix and reinforcement materials used for production. In terms of base matrix, composites are sub-divided into metal matrix composites (MMCs), ceramic matrix composites (CMCs), polymer matrix composites (PMCs).

According to the basis of the matrix;

- Metal Matrix Composite
- Polymer Matrix Composite
- Ceramic Matrix Composite

According to the basis of the configuration of the material;

- Fibrous Composite: This is the case where the matrix is strengthened by continuous or discontinuous fibres, which are in a discrete phase.
- Particulate Composite: In this case, the matrix is strengthened by particles in their discrete phase.
- Laminate Composite

### **2.2.1 Advancement of the composites**

The construction of aircraft components for the implementation of the structure, motor, and composite components has advanced significantly in recent years. Composite materials are increasingly employed in the aerospace sector, owing to their superior corrosion resistance, hardness, and fatigue resistance as compared to other materials. Furthermore, the high running heat of 1400°C has proved that composite materials such as ceramic matrix compounds can meet the increased demand for aviation speeds (Chen et al., 2021).

In recent years, bio-based products have piqued renewed interest as sustainable development strategies expand with the growing concern for the environment. Economical eco-friendly

polymers reduce demand for synthetic polymer manufacture (thus lowering pollution), resulting in a beneficial environmental and economic impact. Biodegradable materials are becoming increasingly popular for application in agriculture, medicine, and other fields. In particular, biodegradable polymer materials (known as bio composites) are of interest (Neto & Nascimento, 2017).

### **2.2.2 Metal matrix composites**

Metal Matrix Composites (MMCs) are becoming a favourable option in a material selection over conventional metallic alloys in many applications. As industrial and commercial applications expand from just aerospace and automobile to marine, defence, recreation, and sporting industries. Metal Matrix Composites (MMCs) are basically a dispersion of ceramic or polymer reinforcement in a metal or alloy matrix (Bodunrin et al., 2015).

Metal Matrix Composites (MMCs) is fundamentally consisting of a metal or an alloy as the continuous matrix or bulk matrix and a ceramic or polymer (organic matter) as reinforcement. MMCs and a reinforcement that can be a particle, short fibre or whisker, or continuous fibre. One of the first developed continuous-fibre MMCs was the aluminium alloy matrix–boron fibre. However, metal matrix composites are divided into three categories based on the type of reinforcement.

- Continuous-fibre reinforced Metal Matrix Composites
- Discontinuous-fibre reinforced Metal Matrix Composites
- Particulate reinforced Metal Matrix Composites (Smith et al., 2019).

### **2.2.3 Polymer matrix composites**

Polymer Matrix Composites are made of organic compounds (polymers) with continuous filaments, laminates, or discontinuous fibres. Supporting reinforcement enables the realization of properties like:

- Stiffness
- Fracture toughness
- High strength (Yogeshwaran et al., 2020).

In recent years, the use of natural fibres as a reinforcing material of polymers has significantly increased. Fibres of environmentally friendly nature such as bamboo and jute are among the high strength fibres used. This rapid development results from the global need for sustainable

material offering better properties than monolithic materials. In one study, Sekaran et al. (2020) investigated the potency of fish scales as support material in polymer matrix composite by varying addition of fish scale powder by wt. %. It was found that at 40 wt. %, maximum tensile strength was greatest is 24.2 N/mm<sup>2</sup>, 30 wt. % for flexure strengths at 63.6 N/mm<sup>2</sup>, and 25 wt. % for impact strengths at 5.5 J.

#### **2.2.4 Ceramic matrix composites**

Solid ceramics have desirable properties, which include good stiffness, constancy at high temperatures and high strength. These desirable properties make them feasible for use in various applications, which include biomedical, aerospace, automobile, industrial, and defence departments. Nonetheless, conventional solid ceramics are apt to be brittle, mechanically undependable and are often, poor conductors of electricity. The need for the improvement of these properties has led to the innovation of ceramic matrix composites. There has been a significant amount of research into the possibility of using fibre-ceramic composites (Porwal et al., 2013).

Ceramic Matrix Composites strengthened with continuous fibres show significant damage and failure behaviours, especially in compression. Ceramics that are strengthened and fortified with continuous fibres can be used in the application of highly high-temperature load-carrying structures (Roebben et al., 1996). Ceramics have good stiffness and thermal stability, making them suitable for use in automobile, consumer, industrial products. However, Ceramic materials are known to be very brittle and hard. An essential method of increasing the strength of ceramics is to reinforce them with fibre, as done in fibre reinforced glass. The reinforcement improves the strength of the ceramic while maintaining its favourable thermal properties.

#### **2.2.5 Applications of aluminium alloys**

Superior mechanical, thermal, electrical and corrosion resistance properties to conventional material have increased aluminium alloy ubiquity in industrial manufacturing in various sectors. Some of those sectors include:

1. Marine sector
2. Automotive sector
3. Construction sector

#### 4. Transportation sector

##### **2.2.6 Marine sector**

Lately, the use of aluminium has extended in the marine vehicle industry because of its light weight and protection from corrosion. 5xxx and 6xxx families of aluminium composites being the most preferred mixtures used in conditions, for example, ocean water which has high material corruption by means of consumption. Composite like AA5083 and AA6082 are applied in the development of ocean vessels.

##### **2.2.7 Automotive sector**

The focal point of vehicle manufacturers has moved in the direction of lightweight materials because of the exhaustion of oil wells leading to coming about expanding interest for eco-friendliness and increased fuel efficiency. In the aerospace industry, aluminium, its alloys, and composites have long been utilized in manufacturing. Also, the aluminium alloy is well established with the combination's grounded plan and assembling strategy, which is all financial, alongside dependable review methods. Similarly, these advantages are sort after in the automotive industry (Jayalakshmi et al., 2016).

Gain such as reduction in overall weight of vehicles makes vehicles more fuel-efficient (Miller et al., 2000). Aluminium castings are applied to many components in the automobile. The engine block material is replaced from cast iron with aluminium alloy to reduce the vehicle's weight to make the vehicle more fuel-efficient (Smith et al., 2019).

##### **2.2.8 Construction sector**

For many years, consideration of required materials advancement and innovation in the construction industry, particularly in third-world countries, diminished the general expense of construction materials (Omoniyi et al., 2021). In these economies, primary construction materials must be affordable. Aluminium sheets are a significant building material constituting about 8 % of the building costs. Roofing materials typically utilized in the construction of industrial buildings and dwellings include aluminium-zinc, and long span aluminium replacing asbestos cement-based roofing. These modern roofing materials are primarily selected for their strength, light weight, attractive surface finish and corrosion resistance, flexibility, light and thermal radiation protection (Adekunle et al., 2020).

### **2.2.9 Transportation sector**

Applications of aluminium metal matrix composites (AMMCs) are growing in the aerospace, automobile, space, underwater environments and transportation industry (Jayashree et al., 2013). Due to its exceptional mechanical strength, great corrosion resistance, and outstanding weldability among Al alloys, 5083 aluminium (Al) has gained a lot of attention as an alternative structural element in railway trains and ships (Ma et al., 2021). Properties of aluminium, like excellent weight strength to weight ratio, ensure improved fuel efficiency. Similarly, its anti-corrosive oxide coating has favoured its use in building vehicles and aeroplanes.

### **2.2.10 Electrical sector**

Aluminium alloy is used in electrical transmission lines. However, possessing a conductivity of less than 64 % of copper. Aluminium alloy excels as in electrical cables due to its:

- Low density: which enables it to be used in overhead cables and still have minimum deflection (sagging)
- Higher ductility: ease of drawing into wires
- Corrosion resistance: preventing it from degrading quickly in corrosive environments (high moisture).

### **2.2.11 Consumer goods**

Metal matrix composites can be customized to have suitable thermal and mechanical characteristics required for enhanced performance of electronic systems and devices. Extensive boron fibre dispersed in aluminium composites is utilized in computer and microcontroller chips as a heat sink in motherboards (Chawla, 2012). Carbon fibres have a high anisotropic thermal conductivity in the fibre direction. Fusing carbon fibres in aluminium composites results in composite material usable in weight reduction applications and heat transfer applications such as high-speed integrated circuit packages (Chawla, 2012).

### **2.2.12 Advantages of aluminium alloys**

Aluminium alloys are non-toxic, making them functional materials for beverages and food containers. Also, aluminium alloys are materials easy to fabricate in various forms, described as having a low degree of workability, a quality appreciated in the industry. It can be rolled, stamped, spun, draw, and formed into complex shapes with ease. AA6061 aluminium alloy are the most versatile form of aluminium alloy used for its weldability, corrosion resistance, good

formability, and strength. Its multi-purpose applications include aircraft, electrical and electronic appliance, fan blades, highway signs, medical equipment, construction material, vehicle parts, railroad vehicles, pipelines and furniture (Davis, 2001).

### **2.2.13 Disadvantages of aluminium alloys**

Aluminium alloys meet design requirements in many industries and applications, making them valuable. However, some aluminium application has faced difficulties in areas relating to weldability of aluminium (Praveen & Yarlagadda, 2005). In real-life applications, the corrosion resistance of aluminium alloy fails to meet many design requirements, such as in the marine industry. The high strength to weight ratio does not favour aluminium over steel as steel has high corrosion resistance in salt water as well as strength.

### **2.2.14 Review of aluminium alloy/synthetic ceramic composite**

It is difficult when producing metal matrix composites to produce a rigid but stiff material to reduce the appearance of cracks and increase static and dynamic characteristics. Hence, there is a need for a suitable selection of reinforcing material and processing conditions (Shirvanimoghaddam et al., 2016). The most common metal matrices utilized for composite material are titanium, zinc, steel, and aluminium (Emara, 2017). While ceramics commonly used as supporting materials include aluminium oxide ( $\text{Al}_2\text{O}_3$ ), silicon carbide (SiC), titanium oxide ( $\text{TiO}_2$ ), graphite (C) and boron carbide ( $\text{B}_4\text{C}$ ), carbon nanotubes produce composites with superior mechanical properties than their monolithic counterparts (Kalel & Patil, 2018).

However, reinforcing metal matrix with ceramics is observed to have some limitations such as high abrasiveness, interfacial de-cohesion, unwanted chemical reaction, recycling difficulties, damaging inconsistencies in expansion of the fused ceramics and metallic materials, high dimensional instability under high cyclic loading, and high cost of ceramic reinforcement material (Alaneme et al., 2019).

Aluminium and its alloys are often used as a metal matrix in composites reinforced with ceramics such as silicon carbide (SiC), titanium carbide (TiC), aluminium oxide ( $\text{Al}_2\text{O}_3$ ) and boron carbide ( $\text{B}_4\text{C}$ ). However, the resulting aluminium metal matrix composites formed are brittle when the ceramic reinforcement content is high. Particle reinforcement is most used due to its relatively low cost compared to continuous reinforcement in the aluminium matrix. Hence, they are commonly called particle reinforced aluminium matrix composites (PRAMCs). Depending on the grain size, components fabricated using PRAMCs experience

high strength to weight ratio, superior tribological properties and corrosion resistance, high specific modulus, and good wear resistance (Kumar & Venkatesh, 2019). Such composites have seen vast amounts of applications in the marine, aviation, and automobile industry.

Kumar & Venkatesh (2019) studied the effect of reinforcing AA7072 with weighing fractions of the ceramic material  $\text{Al}_2\text{O}_3$ , varying from 0 to 9 wt. % using the stir casting method. In comparison to other reinforcement fractions, the AA7072 alloy reinforced with 6% by weight of  $\text{Al}_2\text{O}_3$  shows a considerable improvement in hardness, tensile, and compressive strength. As a result, this combination can be employed in applications that require both lightness and strength. It was discovered that adding  $\text{Al}_2\text{O}_3$  to the alloy matrix enhanced the hardness of the alloy matrix by around 10%.

Kurzawa et al. (2018) investigation on the analysis of ballistic resistance of AC-44200 reinforced with  $\text{Al}_2\text{O}_3$ . Shot materials of 0 %, 20 %, and 40 % vol. of  $\text{Al}_2\text{O}_3$  reinforcement in the Al-alloy manufacture using squeeze casting. Shot materials were subjected to preliminary analysis using ABAQUS, homogenization and simulations. It was concluded that the combination of  $\text{Al}_2\text{O}_3$  particles of the 3-6 microns increases ballistic resistance of the alloy composite compared to non-reinforced alloy. The reinforcement of 20 % of  $\text{Al}_2\text{O}_3$  and 40 % volume fractions cause a 30 % and 60 % reduction in projectile velocity, respectively.

In Zakaria (2014) study of the microstructural and mechanical behaviour of Al/SiC metal matrix composites fabricated using convention powder metallurgical processes. Volume fractions of SiC in Al of up to 15 % at particle sizes of 11, 6, 3  $\mu\text{m}$  studied showed a higher density than that of unreinforced alloy matrix. Similarly, it was found that the corrosion rate of Al/SiC composite material reduced with reduction in particle size and increase in volume fraction of SiC reinforcement in Al-alloy.

The specific strength and wear rate using a pin and disc monitor on AA 6061 matrix titanium carbide particulate reinforced composite, improved wear resistance and specific strength were observed on the increase in weight fraction of titanium carbide present in the composite. The composite was manufactured using the convention stir casting method modified to include two-stage stirring (Gopalakrishnan & Murugan, 2012; Kareem et al., 2021).

Sathish et al. (2020) studied the hardness and wear parameters of silicon carbide, boron carbide, and graphite ceramics reinforced with aluminium LM-30 alloy in weight compositions of 2, 4, and 6%, respectively. Tensile strength was reported to rise with reinforcement up to 4%

reinforcement, then decrease. Similarly, the hardness of the produced composites increased for around 4% before declining. The volume enhances MMC's wear resistance at rapid sliding speed. Sliding causes higher wear rates than unreinforced material, despite its increased hardness. As a result, even a little volume fraction of reinforcement is substantial. Hence a tiny reinforcement volume fraction is significant. The improvement in properties is attributed to the better dispersal of micro powder in the composite.

Mohanavel et al. ( 2018) investigated the mechanical and tribological behaviour of AA7075 when reinforced with aluminium nitride (AlN) through stir casting. The study involved fortification of the AA7075 matrix with 0, 5, 10 and 15 wt. % of AlN by the stir casting process. It was discovered that the alloy matrix grew in tensile strength with an increase in AlN reinforcement weight fractions. Similarly, the fabricated composite displayed greater hardness than the unreinforced aluminium alloy matrix. Finally, an observation made on the composites revealed uniform distribution of reinforcing particles within the alloy matrix.

An experimental evaluation was conducted by Bhaskar et al. (2020) on the wear and mechanical performance of aluminium alloy – ceramic composite, AA2024 SiC, with varying weight fractions of reinforcement (0, 2, 4, 6 wt. %). The density was observed to increase with increasing weight fractions of SiC in composites. Similarly, the tensile strength behaviour of composites varied directly with the amount of SiC reinforcement with the maximum observed tensile strength found for 6 wt. % reinforcement of AA2024 at 202.27 MPa compared to 161.13 MPa in the alloy matrix. The percentage elongation initially reduced as the reinforcing particles increased up to 4 wt. % after which, the percentage elongation began to increase.

Investigation on the corrosion and microstructural properties of Al-MoO<sub>3</sub> was carried out using 5, 10 and 15 wt. % of Molybdenum-oxide of particulate size 10 µm reinforced into aluminium alloy synthesized using powder metallurgy. The study showed that improved corrosion resistance could be attained by increasing the weight fraction of the reinforcing particle, MoO<sub>3</sub>, in aluminium alloy. The composite developed using 15 wt. % MoO<sub>3</sub> in aluminium alloy operated at 27 °C resulted in the lowest corrosion rate of 2.4883 mm/year and corrosion current, 0.000214 A. Also, it was observed that molybdenum oxide formed agglomeration in the alloy matrix. Conclusions were drawn that using MoO<sub>3</sub> as reinforcement caused reduced corrosion rates in composites (Stalin et al., 2020).

More recent research consolidated nano-sized titanium carbide (TiC) with aluminium alloy and investigated the thermal and mechanical behaviour of the resulting composite. Using titanium

carbide nano particles as reinforcement in varying weight volume proportions of 0.5, 1.0 and 1.5 per cent, it was observed that surface roughness reduces with increasing volume fraction of reinforcement, TiC. Also, hardness, young's modulus, tensile, and compressive strength were found to rise with increasing vol.% of TiC. Hence, with 1.5 vol. % reinforcement, a 91.6 % increase in hardness, a 41 per cent increase in young modulus and a 32.9 % increase in compressive strength was attained compared to alloy matrix (Reddy et al., 2018).

Sivakumar et al. (2019) examined the influence of reinforcing mechanically alloyed aluminium with ceramic particles, ZrB<sub>2</sub>, of varying proportions (0, 5, 10 and 20 vol%). Significant improvement was observed on the mechanical properties of the fabricated composite. The hardness improved for increasing reinforcement particles and had improved by 84.3 % (1.51 GPa to 0.94 GPa) in mechanically alloyed aluminium + 20 % ZrB<sub>2</sub> compared to the alloy matrix. Similarly, the compressive strength was observed to rise with increasing reinforcement of the alloy matrix. The coefficient of friction increased slightly for increasing ZrB<sub>2</sub> particles in the aluminium matrix, conversely, wear volume was observed to decrease with an increase in volume fraction of ZrB<sub>2</sub> reinforcements. Hence, the addition of ZrB<sub>2</sub> particles to the matrix resulted in improved wear behaviour.

### **2.2.15 Review of aluminium alloy/biodegradable reinforced materials**

Nowadays, there is a keen interest of the scientific community in the use of biodegradable reinforcement material based on its essential characteristics of being economical, low density, high specific properties, and its relative abundance compared to conventional synthetic reinforcement materials (Bisaria et al., 2015). Biodegradable materials refer to materials that can undergo chemical and physical alteration like transformation or elimination upon contact with living organisms or the biological environment. Recent studies have seen increased usage of agricultural waste as reinforcement material for metal matrix composites to significantly reduce the cost of producing the composites. These waste products include corn stalk ash, bamboo leaf, corn cob ash, corn stalk ash, palm kernel shell ash, and most recently, egg shells (Bodunrin et al., 2015; Joseph & Babaremu, 2019).

In Omoniyi et al. (2021)'s investigation of microstructural and mechanical features of aluminium matrix reinforced with wood particles, stir casting technique was used to fortify the aluminium alloy with varying weight proportions of wood particles (0 % wt., 5 % wt., 10 % wt., 15 % wt., and 20 % wt.). After adding wood particles to the molten alloy, the mixture was agitated at 450 rpm for 1 minute to prevent the wood from burning. Finally, mechanical testing

was performed on the various combinations, and it was discovered that as the percentage of reinforcement increased, the density of reinforcement increased as well. For example, the UTS for a 20 % wt. Al-matrix/wood particle composite was 97.69 MPa, while the UTS for unreinforced aluminium was 40.189 MPa. Similarly, impact energy and hardness were highest when wood particles were added to the aluminium matrix at 10 % by weight. As a result, it was determined that the aluminium matrix reinforced with wood particles, with wood particles distributed equally throughout the matrix, had better mechanical properties than the unreinforced aluminium matrix.

In the synthesis of green metal matrix composite using egg shells (ES) as reinforcement material and its mechanical behaviour examination done by Dwivedi et al. (2016), the Stir casting method was used in fabrication, with argon gas used in the mixture of AA2014 and chicken egg shell to prevent reaction of the matrix with atmosphere. The resulting composite provided a 3.57 % lower density than conventional AA2014 alloy and significantly improved hardness, fatigue strength and tensile strength by addition of 5 wt. % carbonized-chicken ES to AA2014.

Rice husk (RH) is the hard outer coating of the rice crop (paddy grains) separated from during milling from rice grains. The husk is widely available throughout the globe as an agricultural waste product, as about 500 - 600 million tons of rice are produced annually, with 120 million tons of it being rice husk. The most prominent application of rice husk is as a fuel, but it is also used in cement and construction as a mineral additive to improve the behaviour of concrete. Similarly, it is used in the production of steel as an intermediate material in providing insulation properties. RH is a rich source of cellulose and lignin-containing 70 – 90 % of the organic matter. Rice husk ash is produced from the incineration of rice husk by heating to 200 °C for about an hour after washing to remove organic constituents and water. It is then heated to a further 600 °C for about twelve hours to remove carbonic matter. During this transformation, rice husk (RH) changes from a yellowish appearance to a blackish appearance called rice husk ash (RHA). The ash contains over 90 % amorphous silica content, making it a rich source of silica SiO<sub>2</sub> (Singh, 2018; Tiwari & Pradhan, 2017).

In recent years, researchers have attempted to dope it into various materials to create a new class of compounds with improved qualities that can match the current demand from materials. Rice husk ash works as a catalyst in the creation of advanced material due to its abundance and inexpensive cost. Because RHA includes a high amount of silica as a primary component, RHA

has been employed as reinforcement in alloys to improve mechanical properties. For example, the effects of rice husk ash (RHA) reinforcement on Al-Si-10Mg formed via stir casting was investigated by (Saravanan & Kumar, 2013), who discovered that the ultimate tensile strength (UTS) rose as the RHA concentration rose. The composite's ultimate tensile strength rose to 12 % before declining, with compressive strength increasing as the percentage weight of RHA in Al-Si-10Mg rose.

An investigation of the dry sliding wear behaviour of aluminium metal matrix composites prepared using AA 6061 and 0, 2, 4, 6, 8 % weight fractions of rice husk ash reinforcement by compo-casting technique showed that RHA particles improved the wear resistance of composites and reduced damage to the worn surface. The study was carried out using pin-on-disc apparatus at room temperature. RHA particles decreased the wear surface's plastic deformation and the size of the wear debris produced. Increased hardness, the creation of strain fields, homogeneous distribution, the spherical form of RHA particles, and a reduction in effective contact area were all credited with improving wear resistance. With the addition of RHA particles, the wear mode changed from adhesive to abrasive (Gladston et al., 2017). Conclusions can be drawn that using rice husk ash (RHA) as reinforcement material in AMCs results in improved mechanical and wear properties of aluminium metal matrix composites. Moreover, RHA is a cheaper alternative to conventional reinforcement materials such as SiC, Al<sub>2</sub>O<sub>3</sub>, and TiC (Yadav et al., 2018).

A similar investigation was conducted on the microstructural characteristics, mechanical and wear behaviour of aluminium matrix hybrid composites reinforced with alumina, rice husk ash and graphite using particle size rice husk ash and graphite of greater than 50 µm. It was observed that hardness decreased with an increase in rice husk ash and graphite in all composites. The tensile strength and yield strength was also decreased with an increase in weight percentage of alumina and rice husk ash (Alaneme & Sanusi, 2015). Since the reinforcement of biodegradable in metal matrix composites such as AMCs is still in its early phases, several major combinations have still to be investigated. In a study, aluminium alloy with 4.5 % Copper was reinforced with bamboo leaf ash (BLA) fabricated by stir casting method. The resulting composite showed a density reduction with an increase in BLA particles. The hardness of the composites increases with an increase in BLA content compared with the matrix. The maximum hardness was attained at 4 % BLA in the developed composites. Similarly, the tensile strength and yield strength increased with the increasing composition of BLA, as a maximum tensile and yield strength was recorded as 4 % weight fraction of BLA in

the matrix compared to the matrix alloy, 2, and 4 % weight fractions of BLA reinforcement in Al-4.5 % Cu. However, it was reported that when compared to the matrix, the composite's ductility was observed to be lower (Kumar & Birru, 2017).

Since the use of ceramic particles as reinforcement increased density and cost, an exploration of the use of groundnut shells as reinforcement material has been conducted. Groundnut husks are a waste product that pollutes the soil. Dwivedi et al. (2020) analysed the mechanical properties of aluminium hybrid composites reinforced with groundnut shells ash (GSA) and silicon carbide using mixture ratios 10 : 0, 7.5 : 2.5, 5.0 : 5.0, 2.5 : 7.5 and 0 : 10 of GSA and silicon carbide constituting 6 and 10 wt. % of reinforcement. A two-step stir-casting technique was used to fabricate the Al–Mg–Si alloy metal matrix composite. It was observed that hardness and tensile stress increased with a rise in weight per cent of reinforcements, and percentage elongation improved slightly with increasing GSA weight fractions. In addition, as the GSA weight fractions were increased, the fracture toughness improved with a 15.7 % and 7.33 % attained in the 6 wt. % Al–Mg–Si/SiC–GSA, and 10 wt. % respectively.

Further studies were conducted by Bannaravuri & Birru (2018) on the mechanical and tribological behaviour of aluminium alloy consolidated with bamboo leaf ash (BLA). With Al-4.5 % Cu matrix synthesized using varying proportions of the bamboo leaf (0, 2, 4, and 6 wt. %) via stir casting process, the wear rate was observed to decrease with increasing wt.% of BLA particles. However, the minimum wear rate, 31.04 % reduction compared to unreinforced alloy, was identified to occur at 4 wt. % weight fraction of BLA reinforcement in the alloy matrix. SEM (Scanning Electron Micrograph) examination of a worn surface using groove depth revealed that the depth reduced with increasing weight percentages of BLA particles in an aluminium alloy matrix.

Atuanya et al. (2012) performed mechanical and physical properties analysis on bread fruit ash reinforcement in Al-Si-Fe alloy. Using a graphite crucible to stir cast ball-milled bread fruit that had been dried at 1300 °C and turned at 200 rpm for 6 hours, it was discovered density decreased consistently for increasing wt. % of reinforcement reaching a 5.04 % reduction at 12 wt. % reinforcement. Similarly, the impact energy and % elongation has reduced with increasing reinforcement. However, hardness and tensile strength were observed to improve with higher weight fractions of bread fruit ash reinforcement in the aluminium alloy. Later Atuanya et al. (2014) performed an analysis on tribological properties of A356 aluminium alloy reinforced with breadfruit seed ash. The study performed with the same stir casting technique,

adding magnesium to the molten alloy to improve wettability, involved the use of bread fruit reinforcement of varying weight fractions (2, 4, 6, and 8 %) in the alloy matrix. It was discovered that the wear rate of the developed composites decreased with a rise in weight proportions of bread fruit ash in the A356 matrix.

Studies have been directed at adopting eco-friendly reinforcements in metal matrices such as aluminium and its alloys since synthetic composites have shown poor degrees of sustainability both in terms of cost and the environment. However, there are current trends of reinforcing aluminium and its alloys with the ash of leaves and fruits, particularly industrial waste like fly ash. However, these materials are also challenging as they result in burning agricultural produce, releasing some emissions into the atmosphere. Some scientists have worked on other solutions. Hima et al. (2018) reported comparing reinforcing pure aluminium (99.8%) with fly ash particles and aloe vera. By studying the mechanical properties of both reinforcements, they discovered that the density of fly-ash reinforced in aluminium was 2.6 g/cc compared to that of aloe vera being 2.21 g/cc.

Furthermore, the hardness of Al – fly ash (Al-FA) at 28.2 BHN was found to be lower than that of Al – Aloe Vera (Al-AV) at 33.8 BHN. However, there was no significant difference in using aloe vera over fly ash. The ultimate tensile strength of Al-AV was also significantly higher than that of Al-FA at 55.62 MPa compared to 31.44 MPa. The study shows that aloe vera can be used as an eco-friendlier and, in fact, improved reinforcement of aluminium.

Shankar & Elango (2017) reinforced Al-Si-10Mg with proportions of palmyra shell ash, 3, 6, 9, 12 wt. %. The process involved heating the ash to 600 °C to get rid of carbonaceous material. This study discovered that the harness of formed composites increases with an increase in reinforcement material owing to the presence of components like Si, Fe, Ti and K in the ash. Conversely, the density of the synthesized composites reduced with the increase. It was found that the coefficient of friction had reduced with increasing reinforcement, wear rate of formed composite with 12 wt. % palmyra shell ash showed a 9 % lower wear rate than unreinforced aluminium.

Shankar et al. (2018) reinforced Al-Si-10Mg with bagasse seed ash containing 83 % silica (Si) at 6, 9 and 12 wt. %. The formed reinforcement was synthesized using the stir casting process and tested dry sliding pin-on-disc. The composites were observed to have increased in tensile strength continually on increased reinforcement of the alloy with bagasse seed ash from 128.07 MPa in 0 wt. % to 141.97 in 12 wt. % reinforcement. Similarly, the hardness increased with

respect to unreinforced alloy matrix from 14.2 % in 6 wt. %, 23.6 % in 9 wt. % and 33.4 % in 12wt.%. However, the wear rate, impact energy and ductility decreased accordingly. In conclusion, 12 wt. % reinforcement of bagasse seed ash proved to provide the best improvement in the mechanical properties of the alloy.

Arora & Sharma (2018) comparison of the reinforcement of AA6351 with both mono-ceramic composite, silicon carbide (SiC) and rice husk ash (RHA). The hardness and tensile strength were observed to be higher in 8 % wt. SiC reinforcement compared to 8 % wt. RHA reinforcement as 72.5 Hv against 61.3 Hv and 186 MPa against 161 MPa, respectively, both observed to be greater than values obtained for unreinforced alloy matrix. However, the specific wear rate was observed to decreased while density using reinforcement, 8 wt. % RHA was 2.81 % lower than that of unreinforced AA6351.

An evaluation of the mechanical behaviour of AA6063 alloy reinforced with coconut husk ash was done using 3, 6, 9, 12 wt. %. Using the double stir casting process to consolidate the coconut shell ash into AA6063, it was observed that the density of the formed composite had decreased with increasing weight fractions of reinforcement. Similarly, the hardness rose steadily with increasing reinforcement, 35.66HRB at 3 wt. %, 37.28HRB at 6 wt. %, 38.5 HRB at 9 wt. %, and 40.2HRB at 12 wt. %. However, the modulus of elasticity decrease correspondingly and was lower at 12 wt. % observed to be 0.932 compared to unreinforced AA6063, 1.05 (Daramola et al., 2015).

### **2.2.16 Review of hybrid reinforcement on aluminium alloy**

Hybrid composites are materials made by the joining of two or more types of fibre in a material matrix. They give a variety of properties that cannot be accomplished singly by reinforcement and homogenous materials (Chawla, 2012). Especially in mechanical properties, where hybrid composites provide an interface of greater than two working phases delivering more influence of the behaviour of the resulting material alongside the matrix. Prior endeavours at hybridization were made by consolidating stiffer filaments (carbon and boron) with more flexible strands (glass and Kevlar) to improve the strength of the composite and henceforth affecting its properties. Other than improving properties, the joining of glass strands diminishes the expense and increases the resistance of the composite to fatigue.

Currently, SiC, TiB<sub>2</sub>, Al<sub>2</sub>O<sub>3</sub>, B<sub>4</sub>C, all synthetic mono-ceramic reinforcement particles, are used as reinforcement with Al alloys. Some research carried out on hybridizing synthetic with

biodegradable reinforcements such as fly ash, lignite ash, coconut husk has also given better results than single reinforcement (Pawar et al., 2018). Kumar et al. (2018) studied the microstructural, mechanical and wear properties of titanium carbide (TiC), Graphite reinforced aluminium hybrid composites (AHCs). By increasing % wt. TiC reinforcement in aluminium hybrid composite between 1 – 4 wt. %, results showed that an introduction of the TiC particles resulted in an increase in wear resistance, tensile strength and hardness, with maximum values obtained in 4 wt.% Al – TiC hybrid composite.

Umanath et al. (2014) fabricated AA6061alloy based hybrid composites reinforced with both SiC and Al<sub>2</sub>O<sub>3</sub> particles at 25 vol. % using stir casting technique. They found that the micro-hardness of the hybrid composite increase with increasing volume per cent of reinforcement particles. In preparing AA6061/(TiB<sub>2</sub> + Al<sub>2</sub>O<sub>3</sub>) hybrid composite using in-situ processing method between titanium (Ti), boric acid (H<sub>3</sub>BO<sub>3</sub>) powders, and molten aluminium matrix, David et al. (2018) concluded that both reinforcement powders contributed to the enhancement of mechanical properties such as hardness and tensile strength. The mechanical test showed microhardness at 0 wt. % and 15 wt. % to be 60.1 HV and 122 HV, respectively and ultimate tensile stress at 0 wt. % and 15 wt. % to be 160 MPa and 287 MPa respectively.

Kumar (2021) studied the morphological and mechanical characteristics of AA4032 reinforced with granite marble powder and silicon carbide ceramic reinforcement at weight fraction levels 0, 3, 6, 9 % fabricated via stir casting. With reinforcement particle size 54 microns attained, the study revealed that silicon carbide and granite marble particles were distributed uniformly in the matrix of aluminium alloy AA4032, for AMHC samples, up to 6 % reinforcement is observed. The AMHCs appear to have a higher impact strength than the Al-alloy matrix. The impact strength reaches its maximum value at a 3 per cent weight fraction of the reinforcement. Beyond this amount, the impact strength decreases, presumably owing to the composite becoming more brittle as the reinforcing fraction increases.

Liu et al. (2019) carried out tensile strength, compressive strength, hardness, micro-structural and tribological observation on blending of AA7075 with B<sub>4</sub>C and MoS<sub>2</sub>. The reinforcing particles B<sub>4</sub>C was added at 4, 8 and 12 wt. % and lubricant MoS<sub>2</sub> 3 wt. % using stir casting to explored opportunities for the utilization of particle reinforced aluminium hybrid composite in vehicles. By blending AA7075 in 4, 8, and 12 wt. % of B<sub>4</sub>C and MoS<sub>2</sub>, fine dendrites of evenly distributed reinforcement formed in a solution of alloy matrix. The friction coefficient of AA7075 + B<sub>4</sub>C + MoS<sub>2</sub> hybrid composites was in the range 0.48 – 0.49 and was observed to

be greater than that of unreinforced alloy. The tensile strength of the aluminium alloy increased significantly in the reinforcement of  $B_4C$  and  $MoS_2$  compared to unreinforced alloy with maximum values of  $298.52\text{ N/mm}^2$  obtained in  $AA7075 + 12\% B_4C + 3\% MoS_2$  compared to  $221\text{ N/mm}^2$  in unreinforced aluminium alloy. Also, a yield strength of  $172.60\text{ N/mm}^2$  was obtained in  $AA7075 + 12\% B_4C + 3\% MoS_2$  compared to  $95\text{ N/mm}^2$  in the unreinforced aluminium matrix alloy. As deduced, the hardness and compressive strength of the aluminium matrix increased with an increase in the weight fraction of reinforcement. Abrasive wear owing to particle microfracture of the composites was identified as a major wear mechanism for blends of the hybrid composite tested.

A study was carried out on the hardness and erosion-corrosion behaviour of aluminium matrix reinforced with various portions of snail-shell-ash (SSA) and silicon carbide synthesized using stir casting. Maximum hardness was realised at higher reinforcement weigh fractions of the hybrid reinforcement. The composite with a higher hardness value showed enhanced erosion-corrosion resistance. However, the erosion-corrosion resistance in the composites was found to be less than that of unreinforced AA6063 alloy (Aribo et al., 2017).

Using AA3003 reinforced with Carbon Nanotubes (CNT) and titanium carbide (TiC) through the stir casting process, a study was conducted to identify to assess the micro-mechano-tribo behaviours of the newly formed hybrid composite. Using CNT weight fraction fixed at 0.5 % and TiC varying between 0.5 and 2.0 %, it was observed that the density of the composites decreased with an increase in reinforcement particles attaining the lowest density,  $2.95\text{ g/cm}^3$ , at 97.5 wt. % Al + 0.5 wt. % CNT + 2wt. % TiC. Similarly, the hardness of composite varied directly with the weight fraction of reinforcement, TiC, because of the higher interfacial bond between the matrix and reinforcing particles. However, the wear rate of the developed composites was found to be lower than that of unreinforced AA3003 aluminium alloy (Nayim et al., 2020).

Kumar et al. (2020) synthesized composites of aluminium alloy AA6082 reinforced with graphite (Gr) and  $Y_2O_3$  of varying volume proportions, 2 and 6 %, using friction stir casting process to analyse the tribological and mechanical effect of addition of both Gr and  $Y_2O_3$  reinforcement on AA6082. AA6082 reinforced with  $Y_2O_3$  and Gr had an increased microhardness compared to AA6082 matrix alloy by about 40 %. Also, the hybrid composite had higher compressive strength than the unreinforced alloy because of reinforcement particles resisting dislocation in the matrix. The wear rate and friction coefficient were reduced in the

composite compared to the alloy matrix. Both properties were found to be the lowest in AA6082 + 4 % vol. Gr + 2 % vol. Y<sub>2</sub>O<sub>3</sub> than in composite of 6 % vol. Y<sub>2</sub>O<sub>3</sub> and unreinforced AA6082 signifying that graphite was more responsibly for the decrease in wear rate and friction coefficient.

### 2.2.17 Review of chitosan as reinforcement

Advanced composites are commonly employed due to their low weight, strength, stiffness, and toughness. Future materials will undoubtedly enable a wide range of applications, including military, modular building, transportation, food preservation, aerospace, automotive, and biomedical implant technologies, by adopting these features, due to their great wear resistance, high strength-to-weight ratio, and biocompatibility Carlsson et al. (2014).

An example of such a material used in the advanced composite is chitosan (CTS). Chitosan is a yellowish flake-like substance found in decalcified outermost coverings of crabs, lobsters, prawns, and crayfish amongst other aquatic crustaceans, as discover by Hatchett (1799). In recent times, chitosan, which is a naturally occurring polymer like chitin and cellulose is, is obtained from aquatic organisms as well as terrestrial crustaceans, fungi, mushrooms, and mycelia, due to the seasonal variation in the availability of aquatic crustaceans. Chitosan is closely related to the family of polymers chitin sharing D-glucosamine units. However, chitosan is a natural linear polysaccharide and an N-acetyl-d-glucosamine. Still, both polymers possess exceptional properties such as analgesic, non-toxicity, adsorption enhancing, antihypertensive, anticholesterolemic, anticancer, and antidiabetic, thus resulting in its frequent appearance in food, textile, and biomedical products (Ahmed & Ikram, 2017; Crini & Hatchett, 2019; Neto & Nascimento, 2017).

On a molecular basis, chitosan can be divided into low-density chitosan (LDC) and high-density chitosan (HDC). Chitosan properties are greatly affected by purity, solubility, pH, viscosity, hygroscopicity, heat, swelling, reactivity, level of deacetylation. The level of deacetylation is the most paramount property in chitosan. It is known to affect all other properties, especially molecular weight. These properties are essential in creating and extracting chitosan. This report focuses on chitosan gotten from *Micropogonias undulatus* scales and intends to explore its utility as a reinforcement of aluminium metal matrix composites. However, since this strategy is relatively new, a review of previous literature on the use of chitosan in composites is important.

High-density chitosan deacetylated from chitin at a rate of 85 % is used to reinforce epoxy to form nanocomposite using compression moulding technique. The resulting composite was subjected to mechanical and morphological characterization. A combination of the epoxy with 2 wt. % and 4 wt. % of chitosan showed improvements in tensile and flexure strength. However, when a further 2 wt. % of chitosan was added, the composite showed a decline in mechanical properties. Furthermore, Scanning Electron Micrograph revealed a homogenous distribution of the chitosan fillers in the epoxy layers, and a higher weight fraction of reinforcement resulted in more agglomeration (Soundhar & Jayakrishna, 2019).

Khan et al. (2012) studied the mechanical behaviours of cellulose reinforced chitosan nanocomposite film, nanocrystalline cellulose (NCC) to the chitosan polymer which resulted in improved tensile strength. They observed consistently with increasing weight fractions of reinforcement. Morphologically, NCC also enhanced the chitosan's barrier qualities by lowering the VWP and swelling property. The integration of merely 5 % NCC resulted in a 27 per cent reduction in VWP. The study suggests that chitosan/cellulose composite is useful for food packaging.

Gokulalakshmi et al. (2017) did a comprehensive study on the extraction and characterisation of chitosan derived from Catfish. Chitosan is produced via sodium hydroxide deacetylation of the scales. The scanning electron micrograph of the specimen showed thick, rough agglomeration of particles present in chunks with voids between them. It was concluded based on the Infrared Spectroscopy using Fourier transform analysis and X-ray diffractogram that chitosan particles showed antibacterial activities, making them useful for applications in the preservation of food items.

### **2.2.18 Review of the thermal properties and effects of heat treatment of aluminium metal matrix composite**

The manufacturing of metallic alloys could be through the solid phase or liquid. The solid-state manufacturing techniques are mainly powder metallurgy and Additive manufacturing, while liquid-state synthesis of composite includes casting and pressure infiltration. However, beyond the primary synthesis process in the consolidation of reinforcements in matrices, secondary treatment can be employed to attain specific granular or crystalline structures, resulting in enhanced properties or uniformity in the dispersion of reinforcement. Nonetheless, with all substantial research efforts directed towards attaining properties of aluminium matrix

composites, little has been done to adopt secondary treatment alongside the use of the multi-synthesis route (Orhadahwe et al., 2020).

Thermal treatment, also called heat treatment, refers to the use of cooling and heating to alter the properties of a material. Methods that can be treated thermally include normalizing, precipitation, strengthening, tempering, quenching and case hardening (Shrivastava et al., 2019). Structurally, metals consist of a microstructure of crystals (grains) whose arrangement and sizing are integral determinants of the metal's properties. The arrangement of atoms in a crystal structure is called a lattice. This arrangement can be altered by thermodynamic conditions such as pressure and temperature, resulting in allotropic replicas of the metal. With alloys, this morphing results in metallic elements becoming dissolvable in base metals. Hence, intermetallic elements begin to spread within the base metal via diffusion to achieve homogeneity. However, cooling may precipitate the secondary alloying elements and result in grain boundaries formed across the layers. Similarly, Martensitic transformation occurs in materials once a sudden reduction in the temperature of the already heated substance is achieved through varying methods of quenching, where dissolved elements are unable to precipitate from the lattice and are fixated in the crystal structure of the base metals. The resulting allotrope takes on specific properties, which could be harder or softer depending on the material.

The study on the effect of reinforcement on heat treatment on aluminium matrix composite performed on AA6061-T6 reinforced with MoS<sub>2</sub> particles. The fabricated composites were solutionized for an hour at 540 °C, then quenched and age hardened for twelve hours. The heat-treated composites were observed to increase with an increase in tensile and hardness properties above that of the unreinforced alloy matrix AA6061. Conversely, the percentage elongation and flexure strain decrease with increase in reinforcement (Manda et al., 2021).

The heat-treated composites showed the formation of CuNiAl and NiNbAl absent in not treated samples. Similarly, the yield strength was observed to improve on T6 treatment following a gain of 94 MPa and 100 MPa experienced in the AA2024 alloys reinforced with 20 % vol. Ni<sub>60</sub>Nb<sub>40</sub> and 40 % vol. Ni<sub>60</sub>Nb<sub>40</sub> respectively. However, the strain was observed to decrease. Hence, the T6 treatment increased the tensile strength performance of the composes, especially with 20 % vol. reinforcement. Although, heat-treating alloys reinforced with 40 % vol. Ni<sub>60</sub>Nb<sub>40</sub> increased the brittleness of the material (Ertugrul et al., 2019).

The results demonstrate that following solution treatment, the AA061 alloy's peak ageing hardness increases by roughly 66 %. Nevertheless, reinforcing AA6061 alloys with  $\text{Y}_2\text{O}_3 + \text{TiC}$  particles exhibit only a minor improvement in hardness, 15 % to 22 %, under T6 treatment. The formation of precipitates linked to Age hardening treatment of the composites. According to TEM analysis, it is confirmed that numerous needle-like precipitates were observed in the peak-aged AA6061 alloy, which lines up along the  $<100>$  direction of the Al matrix. The presence of precipitates, on the other hand, lacked considerably in the peak-aged AA6061 composites (Chen & Lin, 2017).

Ghanbari et al. (2017) performed annealing and artificial ageing on aluminium metal matrix composite cast using AA2024 alloy reinforced with SiC nanoparticles. The developed composites were subjected to morphological characterisation and hardness tests. The study showed that SiC nanoparticle agglomeration was formed during the friction stir casting process with even distribution of grains coaxially in the stir zone. The hardness of the material increase in heat-treated composites by 70 HV. Thus, the improvement in S-phase precipitate and hardness of the material is a result of heat treatment of the composites.

In the fabrication of  $\text{Al}5\text{Si}1\text{Cu}0.5\text{Mg}/\text{SiC}$ , Li et al. (2019) analysed the influence of solutionizing and ageing on the aluminium metal matrix composite for 9 hours at 520 °C and 6 hours at 175 °C, respectively. The hardness properties of the composite increased from 80.17 HV of unreinforced alloy to 87.06 HV in SiC reinforced alloy and 101.86 HV in the heat-treated composite. Similarly, % elongation grew with the addition of silicon carbide and thermal treatment from 3.81 % for  $\text{Al}5\text{Si}1\text{Cu}0.5$  Mg alloy, 5.23 % for composite, 5.94 % for heat-treated alloy and 6.12 % for thermally treated composite. This culminated in a 60.63 % improvement in percentage elongation. Thus, the solutionizing and ageing of fabricated aluminium matrix composite is responsible for a significant increase in the mechanical strength of the composite.

Jacob et al. (2017) studied the thermal conductivity of AA7075 reinforced with aluminium oxide particles at 5, 10 and 15 wt. % using the laser flash analysis (LFA). The heat conductivity of the fabricated composites increases with an increase in reinforcement from 0 to 10 wt. % reaching a maximum of 129.927 W/mK. However, a further increase in reinforcement by 5 wt. % resulted in a minimum heat conductivity obtained 125.01 W/mK. Thus, it was concluded that further addition of reinforcement particles to AA7075 alloy matrix reduced the thermal conductivity.

In the fabrication of aluminium matrix composites reinforced by carbon nanotubes of 30 $\mu$ m were fabricated by ball-milling; Ogawa et al. (2018) evaluate the thermal conductivity using the laser flash analysis. The thermal conductivity of the composites was developed using CNT1 and CNT2 at 0.5 wt. % resulted in high thermal conductivity of 203.7 W/mK and 186.7 W/mK, respectively. Thus, the composite can be applied in electronic devices such as chipsets requiring thermal management as heat sinks.

A model of the thermal conductivity of diamond reinforced aluminium matrix composite was developed for the theoretical analysis of the thermal conductivity of the composites fabricated using various infiltration techniques. The research found that a higher thermal conductivity was obtained via the gas pressure infiltration technique instead of squeeze casting. However, the study showed a decline in thermal conductivity with the inclusion of reinforcement. Thus, Al-Si was calculated to have 170 W/mK as opposed to Al of 237 W/mK. Thus, it was concluded that Al-diamond developed via gas pressure infiltration technique showed improved thermal conductivity regardless of the addition of Silicon (Chu et al., 2009).

Similarly, aluminium matrix composites reinforced with a hybrid composite mixture of diamond and SiC particles fabricated via gas pressure liquid metal infiltration was evaluated for thermal conductivity. The study showed that by increasing the diamond constituents of the hybrid reinforcement and reducing silicon carbide particles, the thermal conductivity of the composite increased from 220 to 580 W/mK. Thus, predictions and measurements show that silicon content was responsible for the decreasing thermal conductivity in material (Carron et al., 2008).

Nyanor et al. (2021) studied the thermal expansion behaviour of aluminium matrix composite developed using 10 micrometre aluminium reinforced with reduced Graphene Oxide (0.2 to 0.6 wt. %). The presence of carbon nanotubes in the composite were evaluated for influence on the Coefficient of thermal expansion (CTE). The authors discovered that the CTE reduced with an increase in reduced Graphene Oxide content by 28 % in the fabricated composite. The study shows that the reduced Graphene Oxide content was responsible for reducing CTE relevant in automotive applications.

### 2.3 Stir Casting

Metal Matrix Composites (MMCs) manufacturing techniques can be classified into the following:

- Solid-state: processing powder metallurgy and foil deposition
- Semi Solid-state
- In-situ fabrication
- Liquid-state: stir casting, pressure infiltration, squeeze casting, spray deposition, electroplating and electroforming
- Vapour-deposition method (Kumar et al., 2020).

Stir casting, amongst other manufacturing methods like powder metallurgy, squeeze casting, and spray deposition, are applied industrially produces composites. However, compared to other techniques, stir casting is a well-established process for producing MMCs (Ghanaraja et al., 2015). However, the required melting temperature of reinforcement material commonly three times that of the melting temperature of the base metal matrix is a disadvantage of stir casting. Stir casting is still the most economical and widely utilized liquid-state processing technique because it is less expensive than other methods. Stir casting nanocomposites have a high porosity and heterogeneous dispersion of reinforcing particles, making them a good option for making nanocomposites.

Stir casting is a vortex method of producing metal matrix composites. It involves the process of stirring molten metal after the aluminium alloy matrix melts, the molten material is stirred at 500 rpm, and the reinforcement material will be introduced in the formed vortex. The stirring is continued for about 3-4 min (Sharma et al., 2020). Particulate reinforcement in powder form is often dispersed in molten aluminium using a mechanical stirrer. Preceding the mechanical mixing, the surfaces of both alloy and reinforcement should be appropriately cleaned to limit the reaction between these two. The blending of reinforcement particles with molten matrix will capture the particles as well as different contaminations like metal oxide and slag, which forms on the outside of the molten matrix. The formation of air pockets between particles affects the properties at the interface of molten matrix and particles, hindering the wettability between them. In adjusting the interface properties among particles and the softening, and impeding the wettability between them, the vortex method is used to maintain a good distribution of the reinforcement in the molten lattice (Jayashree et al., 2013).

Mehta & Sutaria (2020) investigated the effect of stirring process parameters on the distribution of SiC particles in aluminium alloy LM25. They discovered that the order of importance stirring parameters in the fabrication of composite using stir casting techniques was stirring speed < stirrer position < stirrer blade angle. Having obtained a uniform dispersion at 45°

stirring angle, 400 rpm stirring speed and 40 mm stirrer position. Gopalakrishnan & Murugan (2012) reported creating aluminium alloy reinforced with titanium carbide (Al-TiC) using an enhanced stir casting method. Using SEM analysis, they determined that a defect-free composite was made by melting AA6061 via two-step mixing process by employing magnesium addition to increase wettability of TiC with AA6061 at interface of both materials. Thus, with increasing percentages of TiC added, the composite's specific strength has improved.

## CHAPTER THREE

### 3 MATERIALS AND METHODOLOGY

#### **3.1 Introduction**

It has recently been discovered that aluminium metal matrix composites possess desirable properties physical and mechanical that is advantageous in applications in various industries such as automotive/automobile, aerospace, marine, etc. Varying problems arising in the aforementioned sectors and industries have made it necessary for the development of materials with specific properties. Reinforcements will bolster some of these properties already possessed by aluminium and develop new ones relevant to the application in respective industries. This chapter provides details on the methods used to develop these new materials and the safety measures taken during the process.

#### **3.2 Materials**

##### **3.2.1 Workpiece**

AA 6061, aluminium alloy, with composition provided in Table 3.1 has a very high percentage of aluminium at 97 % and relatively lower proportions of other metals: silicon, Si; manganese, Mn; zinc, Zn; chromium, Cr; copper, Cu; magnesium, Mg; and iron, Fe. The least of which is titanium by weight per cent as the alloy is composed of just 0.13 % of the element. The primary alloys in the composition are silicon and magnesium.

Aluminium 6061 alloy is the primary phase or the primary metal employed in this project. Aluminium 6061 is a magnesium-silicate alloy with minor iron, copper, chromium, zinc, tin, and manganese. Silicon and magnesium are the primary alloying constituents of aluminium 6061. Due to its desirable features, such as high strength and weldability. It is also inexpensive and readily available, in addition to those features. Similar alloys, aluminium alloy 1100 (AA 1100), aluminium alloy 5052 (AA 5052), aluminium alloy 3003 (AA 3003), and other aluminium alloys, are suitable replacements for AA 6061 in this experiment. Table 3.1, Table 3.2, and Table 3.3 reveal the chemical, mechanical, and physical properties of aluminium alloy 6061.

**Table 3.1: Chemical Composition of AA6061**

Component	Weight (%)
Al	97
Si	0.5
Mg	1.0
Cu	0.3
Cr	0.25
Mn	0.14
Ti	0.13
Zn	0.22
Fe	0.5

**Table 3.2: Mechanical Properties of AA6061**

Properties	Metric
Ultimate Tensile Strength	6400 KN
Elongation at Break	2.4 %
Hardness, Brinell	110.69 KN

**Table 3.3: Physical Properties of AA6061**

Property	Metric
Density	2.7 g/cm <sup>3</sup>

### 3.2.2 Reinforcement

The substances selected for reinforcement were chosen by considering their properties and their distinct or particularized purpose. Chitosan was chosen as the reinforcing matrix in this research paper with a particle size of 90 µm using weight fractions of 0 %, 3 %, 6 %, 9%, and 12 %. The reasons for this selection are as follows;

- It has appealing properties like high thermal conductivity, high tensile and hardness strength
- Chitosan possesses biogenic antibacterial properties.



**Figure 3.1: Dried *Micropogonias undulatus* scales**

### 3.2.3 Reinforcing technique

The composites used for the analysis were created using stir casting, a liquid state reinforcing technique. Stir casting involves mechanically stirring molten metal of the base matrix to form a vortex and introducing reinforcement particles into the mixture. It is an economical way to achieve a homogenous distribution of reinforcement particles in a bulk matrix. Also, this cost-effective liquid phase fabrication technique has straightforward procedures and permits modification of the technique to attain desired chemical and physical properties for the synthesized composite. Furthermore, the stir casting technique can be conveniently employed in the mass production of composites in the industry.



**Figure 3.2: Stir casting furnace**

#### **3.2.4 Scanning electron microscope (SEM)/ Energy dispersive spectroscopy (EDS)**

Scanning electron microscopy (SEM) is a technique for obtaining three-dimensional, high-resolution images of a sample surface, which provides information about the substrate's surface shape, content, and topology. It delivers strong magnification and graphic surface patterning by using a concentrated beam of electrons to collect visual information of the sample. Energy Dispersion Spectroscopy (EDS) is a systematic method for determining the constituent constituents of samples in chemical microanalysis. The EDS method detects X-rays emitted from materials during continuous flow by an electron beam, which is utilized to obtain elemental identification and quantitative constitutional data for the capacity under investigation. The scanning electron microscope used in the study is shown in Figure 3.3.



**Figure 3.3: Scanning Electron Microscope**

### 3.2.5 X-ray diffractometer (XRD)

The X-ray Diffractometer (XRD) is a crystallographic analysis instrument, which provides quick quantitative phase analysis. It is used to determine and identify the number of crystalline phases in a mixture. Since Crystalline structures diffract X-rays, hence the use of this technique for analysing crystalline materials and providing details on phases, structure, orientation, grain size, and defects. These techniques can be performed in various ways, including:

- X-Ray Powder Diffraction: In this method, the sample is ground to powder, and the grains of bulk crystalline material is studied as randomly oriented in the sample. It is the most popular technique.
- Single-Crystal X-ray Diffraction: This method involves obtaining details such as bond angle, cell dimensions, site ordering and bond length on the inner lattice structure of a single crystal.

The XRD pattern for individual structure is therefore unique to a material and distinguishable from others. The pattern provides information on the atomic composition of crystalline materials. The diffractometer utilised for this study uses Cu  $\text{K}\alpha$ , as the source of x-ray, at 40 KV and 20 mA. Diffractometer results should indicate the phase composition of material showing scattering peaks corresponding to the various d spacings in the crystal lattice. The positions and the intensities of the peaks are used to identify the material's underlying structure

(or phase). The diffractometer is operated by projecting an incident x-ray toward the sample. This results in constructive interference and a diffracted ray. Once the conditions of diffraction are determined to obey Bragg's Law:

$$n\lambda = 2d \sin \theta \quad (3.1)$$

- $d$  is lattice spacing
- $\lambda$  is the wavelength
- $n$  is the order of the diffraction
- $\theta$  is the angle of diffraction in degrees,

the diffracted rays are counted. Then, a range of 2 theta angles is scanned to obtain all possible directions of diffraction as the material is randomly oriented in powder state. The X-ray detector plots the diffractogram of the peak intensity and the 2-theta angle. The Analytical X'Pert High Score® software with (ICSD) build-up database was used to identify the phases from the d-spacing, which is obtained from the conversion of diffraction peaks. The XRD machine utilized in this experiment is shown in Figure 3.4.



**Figure 3.4: X-Ray Diffractometer**

### 3.2.6 Micro-hardness tester

For this study, the Brinell Hardness Tester was used to determine the Brinell hardness values. The Brinell hardness tester is used to test materials with a coarse appearance or an exterior that is not polished enough to be tested using conventional methods. The Brinell hardness testing typically uses a high-test load of around 3000 kg and a 10-mm-diameter indenter. This is done

to ensure that the indentation results outperform most surface and sub-surface incompatibilities. It resists plastic deformation when indentation occurs. Hydraulics are used to operate the machine. The hardness was measured for 15 seconds at a mass of 100 g, and the depression detected was measured using a Brinell microscope across a minimum of two normals (at right angles to each other) diameters, and the results were estimated. The Brinell hardness number is calculated using equation 3.2.

$$BHN = \frac{2P}{\pi D(D - \sqrt{D^2 - d^2})} \quad (3.2)$$

Where;

P = load applied (KN)

D = diameter of intender (mm<sup>2</sup>)

d = diameter of indentation (mm<sup>2</sup>)

### 3.2.7 Tensile testing machine

The tensile tests were performed using the Universal testing machine (UTM) SM1000. The tests are used to determine the tensile and compressive strengths of materials, as well as elasticity, yield strength, and bond compression. It can be used to perform a variety of compressive and tensile tests on a variety of materials, including metals, concrete, and rubber, as its name suggests. The load capacity of this machine ranges from 5 kN to 2000 kN. When the test sample is positioned between the machine's clasps, the device works. The force is recorded by the machine after the test sample has been subjected to a tensile test; this occurs as the load is applied to the test sample. Each sample's length difference is also calculated.

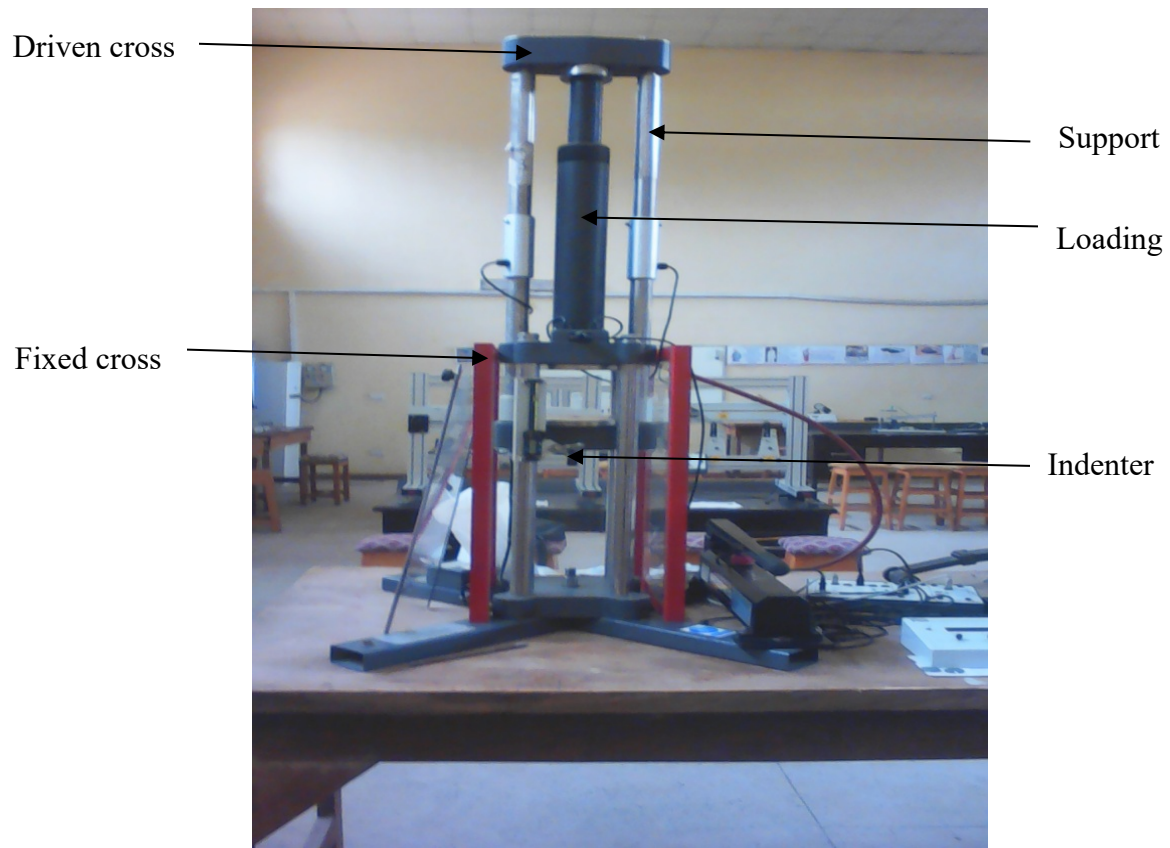


**Figure 3.5: Universal Testing Machine**

### 3.2.8 Cutting machine

The electrical cutting machine was used to cut, shear, or shave the aluminium metal. The machine is totally automated and does not require any operator intervention during the machining process.

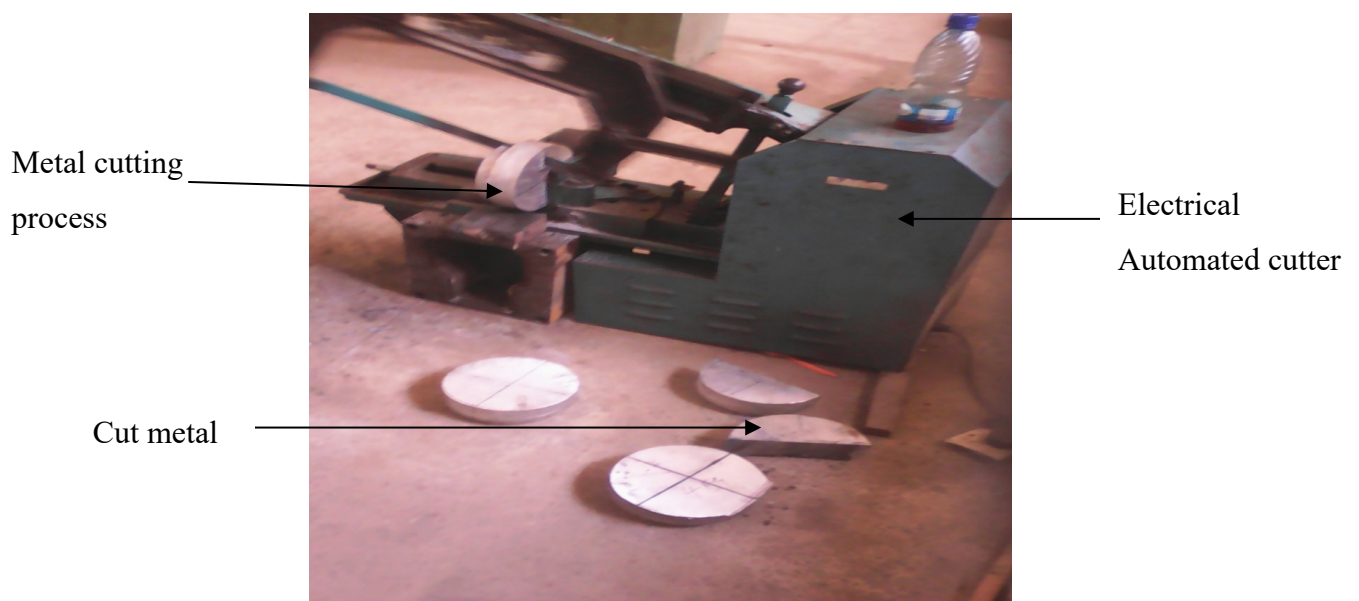


**Figure 3.6: Cutting Machine**

### **3.2.9 Electrical analytical weighing balance**

The masses of small samples are weighed in grams using an electrical analytical balance. The weighing dish is placed in a clear airtight container to prevent dust and air from interfering with the experiment's results. The weighing balance used was the OHAUS Pioneer™ PA214 Model.



**Figure 3.7: OHAUS PioneerTM PA214 Model**

### **3.2.10 Electrical properties testing**

The ammeter-voltmeter technique was used to investigate the electrical characteristics of the cast composites. This is the most straightforward and quick way of determining electrical resistance. Over a wide range of resistances, it provides an accurate value. As indicated in Figure 3.8, the samples were cut into dimensions of 20 x 10 x 5 mm and connected in a circuit using a voltmeter and an ammeter. This setup enables the measurement of the resistance of the material and the amount flowing through the material once voltage is applied. Hence, the resistivity property of the developed composites can be determined.

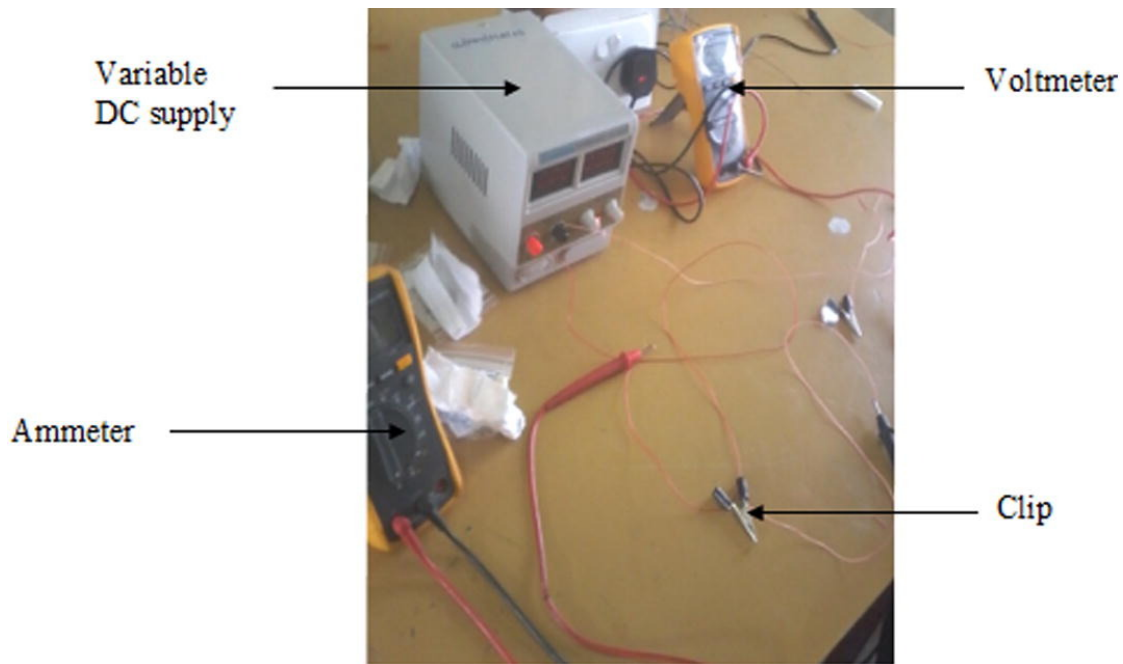


**Figure 3.8: Electrical properties testing experiment setup**

### 3.2.11 Thermal properties testing

A non-contact thermometer (Raytek-MT4) having the least count of  $0 \geq 1^{\circ}\text{C}$  with an accuracy of  $\pm 2\%$  was used to measure temperature readings from the surface of the fabricated composite, the greenhouse temperature. Similarly, a digital hygro-thermometer (model: Lutron HT-3003) with the least count of 0.1 % was used to measure the relative humidity inside the lab, while an electronic weighing balance was used to measure the weight of the samples. The experimental setup evaluated the physical properties of air under forced convection against the samples. Therefore, an electronic digital anemometer was used to measure the air velocity across the lab section during the forced convection. Also, the Temperature values measured were ambient air temperature,  $T_a$ ; and surface temperature of composite,  $T_g$ , using alcohol glass bulb filled thermometers.



**Figure 3.9: Thermal properties testing experiment setup**

### 3.3 Material and Methods

#### 3.3.1 Sectioning

The aluminium alloy, AA 6061, used in this study was purchased from a metallurgical vendor. An automatic metal cutting machine was used to dissect the samples into sections. Using soluble oil as coolant and lubricant, metal distortions and heat in the developed composites were mitigated. The resulting sections were those of 97, 94, 91 and 88 per cent by weight proportion, respectively.

#### 3.3.2 The proportion of reinforcing particulate

After collecting the fish remains in the school cafeteria and kitchen, the scales were dried for three days. Once the scales had dried properly, they were ground into powder using an industrial grinding machine. The powdered chitosan were sieved to obtain filtrate of particle size 90  $\mu\text{m}$  (microns). 90  $\mu\text{m}$  particles of chitosan were measured into different proportions of 3, 6, 9 and 12 g, respectively.

### **3.3.3 Preparation of reinforced aluminium composite**

Next, the samples of both matrix and reinforcing particles were taken to the foundry for stir casting of the aluminium matrix composite. Measured sections of aluminium alloy, AA6061, 97, 94, 91, and 88 g, were placed in a graphite crucible and melted at 810 °C using a pit furnace. Then, magnesium was inserted into the molten aluminium as a wetting agent. Similarly, powdered 90 µm sized chitosan were heated to 700 °C for an hour. Finally, the particulate reinforcements, chitosan, was introduced into the molten aluminium alloy using a graphite stirrer for unvarying circulations.

### **3.3.4 Characteristics of reinforced aluminium composite**

Microstructural analysis and observations were carried out using the X-ray diffractometer and Scanning Electron Microscope to observe new phases developed in newly synthesized alloy composites due to the introduction of reinforcements. Similarly, mechanical characterisation was carried out using the universal testing machine and Brinell's hardness tester.

### **3.3.5 X-ray diffractometer (XRD)**

The X-ray Diffractometer (XRD) is employed to analyse the structure of sample composites to recognize their composition. A scanning point was located between the radiation source and detector with a start angle of 20 ° up till 90 °. The observation from the diffractometer holds details on the compositing elements deposited in the structure of the composite. Hence, XRD can be used alongside other microstructural characterization means to provide knowledge on the property-structure behaviour of the composites. The following are prescribed processes applied:

- The powdered AA6061/90-micron chitosan samples are gently pressed into an aluminium sample holder till flush with outside rim and measured through a wide-angle Phillips P.W. 1011 goniometer connected to a PM 8220 recorder.
- The scanning was done from 2 ° to 40 ° under the following instrumental setting conditions.
- Nickel filtered Fek and radiation
- Recording/scanning rate = 1 ° 20 cm/min.
- Time = constant 4.

- Range = 4 x 10 C.P.S
- Voltage is 28 kv/12 mH
- The interpretation of the diffractograms was made by using the reference conversion table to 20 to d-values for the Fek alpha radiation to the JCPDC manual (1972).

The XRD facilitates our recognition of the blend of particles present in the reinforced composite. It yields a bit of the essential information needed to ascertain what deposits will be derived from the addition of reinforcement. It augments other characterization techniques, including optical/light microscopy and scanning electron microscopy, for improved know-how of the behaviour of property structure. The scanning point was situated between the X-ray source and a detector, and the start angle was between 20 ° through 90 °.

### **3.3.6 Scanning electron microscope**

A scanning electron microscope was used to investigate the physical and mechanical structure, as well as the grain quality of the reinforcing particle injected (SEM). By observing the interface between metal and reinforcement, a focused electron beam was used to obtain optical data and observe the microstructural arrangement of the composite samples, as reported in section 3.2.4 of this chapter.

### **3.3.7 Microhardness testing**

In obtaining the estimated hardness of the different composites, a spherical indenter is utilized to create impressions. These impressions are made in equidistant dimensions at the interface. The microhardness of the sample is determined using 100 micro-meters spacing between indentations utilizing a 100 g load for a 15-second dwell duration using Brinell's optical methods to assess the impression size.

### **3.3.8 Tensile testing**

As a part of mechanical characterization, tensile strength tests were conducted using the Universal Testing Machine SM1000. The samples underwent leading of 100KN (10 Tons) and deformed till fracture. At the fracture point, the strength is recorded to determine the percentage of elongation.

### 3.3.9 Electrical properties testing

With the sample connected across a voltmeter by means of a crocodile clip, as shown in Figure 3.10, the DC supply Voltage was varied in steps of 0.2 V. Then, the current is measured via an ammeter of range 5Ampere. The Current and Voltage obtained are tabulated against each other, and the mean resistance of the samples are derived via linear regression technique. Next, the resistivity is computed using the formulae 3.3, 3.4 and 3.5. Finally, the conductivity is then found to be the inverse of the resistivity.

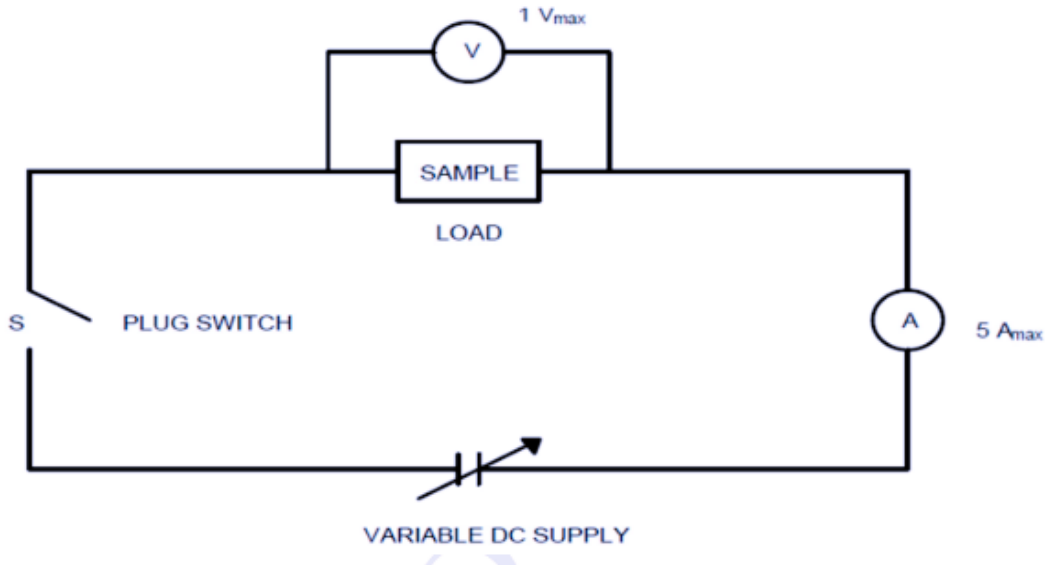


**Figure 3.10: Electrical properties testing experiment circuitry**

$$\text{Resistance, } R = \frac{V}{I} \quad (3.3)$$

$$\text{Resistivity, } \rho = \frac{RA}{l} \quad (3.4)$$

$$\text{Conductivity, } G = \frac{1}{\rho} \quad (3.5)$$

Where;

V = Voltage in V (Volts)

I = Current in A (Ampere)

R = Resistance in  $\Omega$  (Ohms)

$\rho$  = Resistivity in  $\Omega\text{m}$  (Ohm-meter)

G = Conductivity in S/m (Siemen per metres)

### 3.3.10 Thermal properties testing

In obtaining the thermal properties of the developed composite, measurements taken on the temperature are tabulated and evaluated to obtain the convective heat transfer coefficient using the formulae 3.5, 3.6, 3.7 and 3.8. In formula 3.5, variables C and n are evaluated using linear regression in (3.7). Furthermore, the obtained physical properties of air were employed in calculating the Nusselt number. Nusselt number is the ratio of convective heat transfer to conductive heat transfer (Roy & Roy, 2020). Hence, using the Prandtl number of air to be 0.69 (Patience, 2013), at boundary conditions of fluid flow, Re (Reynold's number) as  $5 \times 10^5$  the conductive heat transfer coefficient of the unreinforced alloy, and composites fabricated with (3, 6, 9, and 12 wt. %) chitosan is computed.

$$Nu = \frac{hX}{K} = C(Re * Pr)^n \quad (3.5)$$

$$Z = 0.016 * \frac{K}{X} (P(Ta) - \gamma P(Tg)) At \quad (3.6)$$

$$\ln\left(\frac{m}{z}\right) = n \ln(Re, Pr) + \ln(C) \frac{hX}{K} \quad (3.7)$$

$$h = \frac{K}{X} C(Re * Pr)^n \quad (3.8)$$

Where;

Ta = ambient temperature inside greenhouse ( $^{\circ}$ C)

Tg = surface temperature of composite in the lab ( $^{\circ}$ C)

Pr = Prandtl number of air

Re = Reynolds number of air

m = mass evaporated evaluated (kg)

$\gamma$  = humidity in percentage (%)

h = convective heat transfer coefficient ( $W/m^2 \text{ } ^{\circ}\text{C}$ )

K = conductive heat transfer coefficient ( $W/m \text{ } ^{\circ}\text{C}$ )

### 3.4 Conclusion

Experiments performed in this chapter are done with accurate instruments, and results will be discussed in the next chapter.

## CHAPTER FOUR

### 4 RESULTS AND DISCUSSIONS

#### 4.1 Introduction

The increasing awareness in the modern civilisation to synthesize composite material coupled with a universal drive for sustainability has propelled researchers to explore reinforcement of alloys with agricultural waste products (Ghanbari et al., 2017b). These experiments have led to substantial development in industries such as in. the results of these experiments inform engineers and designers on in the selection of improved materials over their conventional counterparts. Similarly, this research explores the heat treatment of aluminium alloy (AA 6061) reinforced with an agricultural waste polymer material, chitosan, in varying mass proportions. The study results involving various characterisations, analysis and testing of the fabricated composites are provided in section 4.2 (Aigbodion et al., 2021).

#### 4.2 Aluminium Reinforcement with Chitosan

The weight fractions for reinforcing aluminium alloy (AA 6061) reinforced chitosan is showing in Table 4.1. as weight proportions of chitosan (reinforcement) and AA 6061 (base matrix).

**Table 4.1: Reinforcement Weight Parameters**

Sample designation	Weight of Chitosan (%)	Weight of AA6061 (%)
AA 6061	0	100
AA 6061 + 3wt.% Chitosan	3	97
AA 6061 + 6wt.% Chitosan	6	94
AA 6061 + 9wt.% Chitosan	9	93
AA 6061 + 12wt.% Chitosan	12	88

##### 4.2.1 Microhardness analysis of chitosan reinforced aluminium alloy AA6061

The effects of the introduction of chitosan at varying weight proportions into the aluminium alloy matrix on the hardness of the material are shown in Figure 4.1. Pure AA 6061 alloy has a hardness value of 55.2 HRB. This value is suitable for its selection in piston design in gasoline and diesel engines of automotive (Udoye et al., 2019). However, the addition of chitosan at 3 wt. % to AA60601 matrix provided an observed hardness value of 57.4 HRB, which corresponds to a 3.99 % increase in micro-hardness compared to the unreinforced alloy.

Similarly, additions of 6 and 12 wt. % provided microhardness values of 59.2 and 60.2 HRB; 7.25 % and 9.06 % hardness improvements from unreinforced alloy. An anomaly was observed in the sample, aluminium matrix composite reinforced with 9 wt. % chitosan, the micro-hardness value for this sample 57.8HRB showed improvement in microhardness from 3 wt. % by only 0.7 % and unreinforced alloy by 4.71 %. However, the 9 wt. % reinforcement sample performed less than that of 6 wt. % chitosan reinforcement by 2.36 % in the hardness test, which might be due to slight errors in fabrication. The result obtained established the correspondence of increase in reinforcement with an improvement in the mechanical property, hardness.

Comparably, AA6063 reinforcement of with calcium-rich particles  $\text{CaCO}_3$  showed an increase in the hardness property between 55 to 70 BHN with 2 to 6 wt. % of  $\text{CaCO}_3$  (Adeodu et al., 2020). Similarly, the developed composites in this experiment, which have high Calcium composition, show improved hardness of up to 9.06 %, hence, well suited as a replacement material for piston production based on mechanical hardness.

**Table 4.2: Hardness test result of samples**

Sample	Hardness (HRB)
AA 6061	57.4
AA 6061 + 3 wt. % Chitosan	59.2
AA 6061 + 6 wt. % Chitosan	57.8
AA 6061 + 9 wt. % Chitosan	60.2
AA 6061 + 12 wt. % Chitosan	55.2

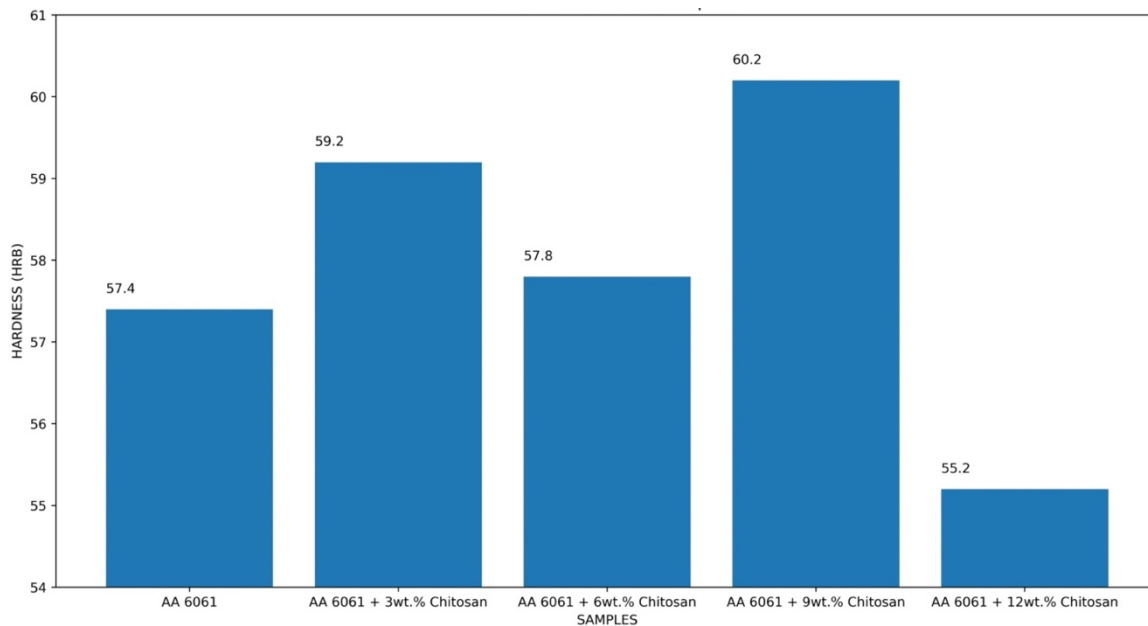


**Figure 4.1: Hardness test result of samples**

#### **4.2.2 Ultimate tensile strength for the chitosan reinforced AA6061 and unreinforced AA6061**

The fabricated composite is aimed at being potential replacements for conventional usage of just aluminium alloy in industries such as automotive, aerospace and construction. In these industries, key components such as pistons (automotive), turbine blades (aerospace), chassis (automotive and aerospace), door frames and windows (construction) are frequently subjected to immense axial loading leading to tensile stress formed in the material. This section describes using figures and tables the results of tensile tests conducted on the developed metal matrix composites using the Universal Testing Machine (UTM SM1000).

**Table 4.3: Showing the maximum stress of the control sample**

Specimen	Length (mm)	Diameter (mm)	Maximum Tensile stress (MPa)
1	30.000	4.000	83.073

**Table 4.4: Showing Tensile Stress at Break of the unreinforced specimen**

Specimen	Load at max. tensile stress (N)	Tensile strain at max.	Tensile extension at tensile stress	Energy at max. tensile stress (J)	Tensile stress at Break (MPa)
1	1043.92590	0.02334	0.70019	0.13314	63.436

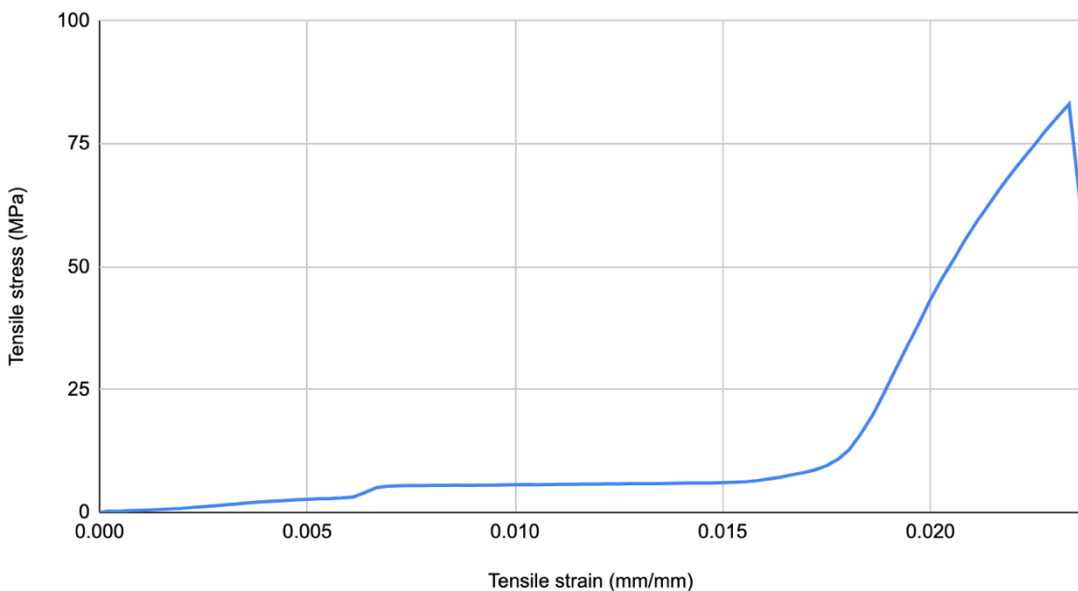


**Figure 4.2: Showing Tensile Strength of unreinforced AA6061 alloy**

In this section, specimen 1 refers to AA6061 + 3 wt. % chitosan, specimen 2 to AA6061 + 6 wt. % chitosan, specimen 3 to AA6061 + 9 wt. % chitosan, specimen 4 to AA6061 + 12 wt. % chitosan.

**Table 4.5: Showing the maximum stress of the reinforced specimens**

<b>Specimen</b>	<b>Length (mm)</b>	<b>Diameter (mm)</b>	<b>Maximum Tensile stress (MPa)</b>
1	30.00	4.00	81.85
2	30.00	4.00	7.40
3	30.00	4.00	111.96
4	30.00000	4.00000	114.91521

**Table 4.6: Showing Tensile Stress at Break of the reinforced specimens**

<b>Specimen</b>	<b>Load at max tensile stress (N)</b>	<b>Tensile strain at max tensile stress (mm/mm)</b>	<b>Tensile at max tensile stress (mm)</b>	<b>Energy at max tensile stress (J)</b>	<b>Tensile stress at break (MPa)</b>
1	1028.60	0.02	0.70	0.15	81.85
2	93.05	0.02	0.68	0.04	6.12
3	1406.90	0.019	0.57	0.15	111.39
4	1444.07	0.027	0.81	0.21	114.92

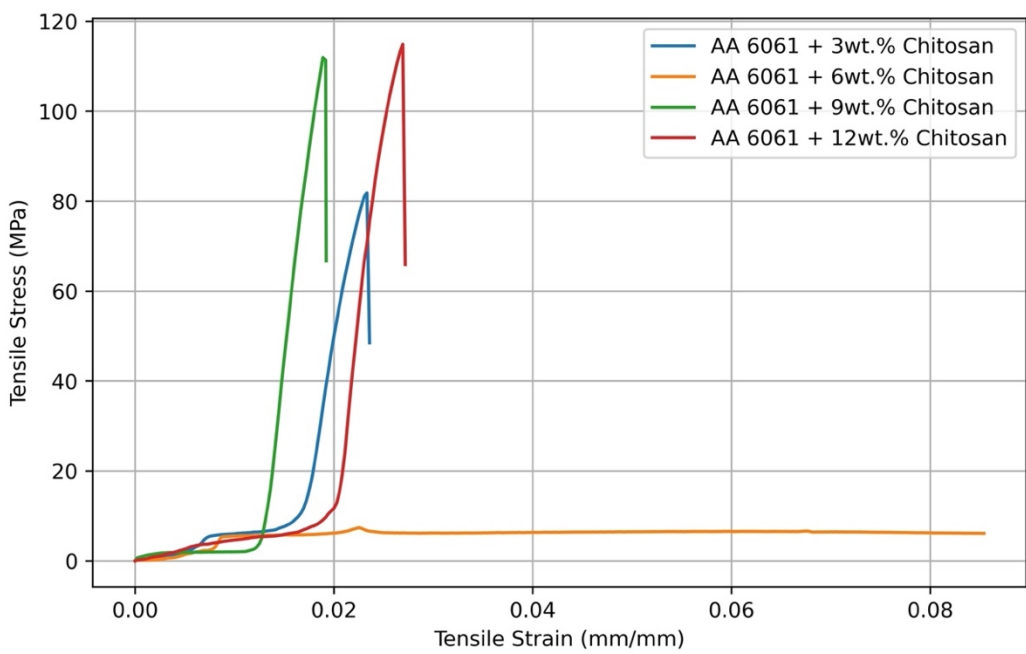


**Figure 4.3: Showing Tensile Strength of the reinforced Al6061 alloy matrix composites**

Figure 4.2, Figure 4.3, and Table 4.4 show the maximum tensile strength of unreinforced aluminium alloy (AA6061). Figure 4.3, Table 4.5, Table 4.6 show tensile strength of aluminium matrix composite fabricated by consolidating chitosan at varying weight fractions into the AA6061 matrix. It is observed that the addition of chitosan as a reinforcement particle improve the maximum tensile break strength of the material as observed in 3 wt. %, 9 wt. % and 12 wt. % of reinforcement. Furthermore, an improved maximum tensile strength is observed in samples of 9 wt. % and 12 wt. % reinforcement having values of 111.95784 MPa and 114.91521 MPa, respectively, compared to 83.07299 MPa. This represents an approximate 25.80 % and 27.71 % improvement in tensile strength, respectively. However, an anomaly is observed in the sample with 6 % reinforcement with 7.40458 MPa. It showed no significant improvement in tensile strength with the addition of chitosan. Correspondingly, AA6061 reinforcement with agro-waste rice husk ash nanoparticles via stir casting, Aigbodion et al. (2021) showed improvements at a similar rate.

#### 4.2.3 Scanning electron microscope and Energy disperse spectroscopy analyses

Morphological analysis was performed using Scanning Electron Microscope on unreinforced aluminium alloy and the composite specimens fabricated with reinforcements of chitosan at

varying weight fractions. Preparation of the materials involved grinding on emery paper. Also, the sample to be metallographically examined was polished on a fine polishing machine to ensure appropriate results.

### I. SEM/EDS of unreinforced aluminium specimen

Figure 4.4 shows a micrograph of the pure control sample. The SEM sample image was taken at 35000X magnification and at a working distance of 20  $\mu\text{m}$ . From this image, voids and grain boundaries are observed, and SEM reveals the crystal arrangement of aluminium alloy with other trace elements. The EDS reveals the constituent element of the unreinforced aluminium specimen. The control sample was further studied using EDS. The EDS scale showed the supremacy of silicon, calcium, oxygen, alumina with other essential constituents. The EDS result established the constituent elemental structure of aluminium alloy, as shown in Figure 4.4.

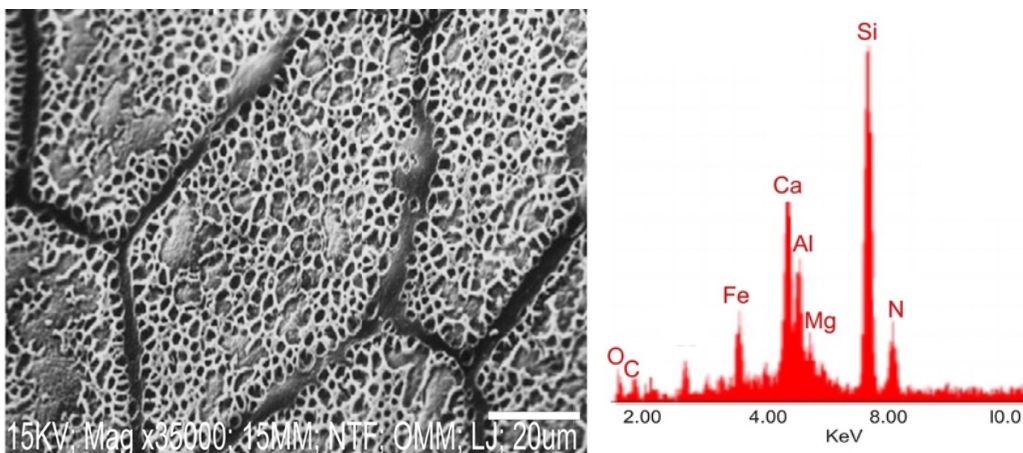


**Figure 4.4: (a) Micrograph of Control Sample AA6061. (b) Energy Dispersive Spectra Showing the Mineral Content of Control Sample AA6061**

### II. SEM/EDS of reinforced Al6061 with 3 wt.% chitosan

In Figure 4.5 a and b, the scanning electron micrograph of the composite, AA6061+ 3 wt. % chitosan, is shown. The micrograph image is obtained at configurations: 35000X magnification with an acceleration voltage of 15 kV and a working distance between 20 and 100  $\mu\text{m}$ . From the SEM, fibrous particles of approximately 0.2  $\mu\text{m}$  thick are inoculated in the matrix. Furthermore, it is observed that there is uniform dispersal of particles in the composite matrix with little voids of 2.6  $\mu\text{m}$ . The rich fibrous particles dispersed in the matrix increase the tensile strength of the composite material by transferring strain evenly to the alloy matrix. The Energy

Disperse Spectroscopy chart shows that the composite is rich in calcium, silicon, oxygen, alumina, and carbon and contains sparingly amount of Iron and Magnesium elements.

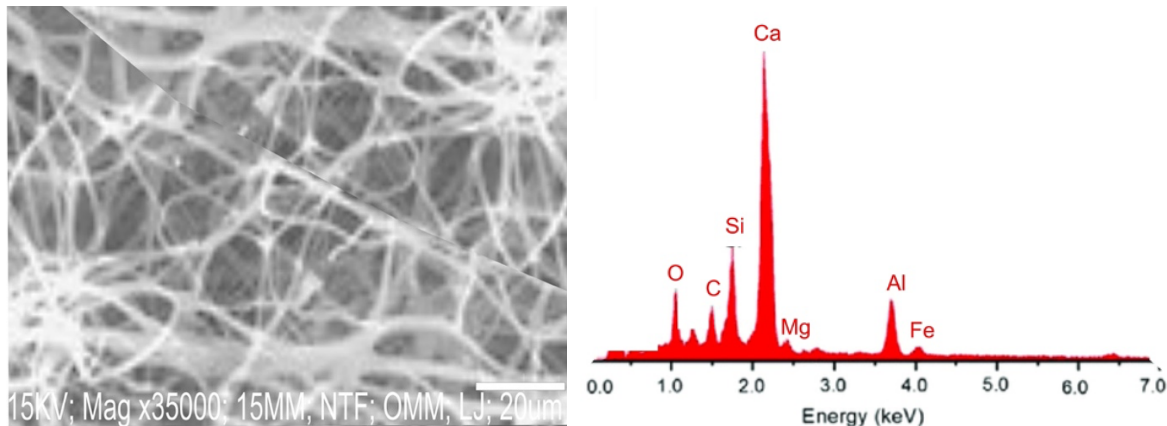


**Figure 4.5: (a) SEM image of AA6061 + 3 wt. %Chitosan. (b) EDS of specimen**

### III. SEM/EDS of reinforced AA6061 with 6 wt. % chitosan

Figure 4.6 a and b represent the scanning electron micrograph (SEM) and energy dispersion spectroscopy (EDS) image of the composite, AA6061+ 6 wt. % chitosan, is shown. The micrograph images were obtained at configurations: 35000X magnification with an acceleration voltage of 15 kV and a working distance of 100 μm. The SEM shows a tightly packed morphological structure like that of a fish scale with linking reinforcements within the grain boundaries. The structure is a result of uniformly dispersed with no voids in the material because of forced vortexes during stir casting. Furthermore, the structure represents a strengthened composite thus would provide an improved response to mechanically loading in form of tensile or hardness as a result of the reinforcing links within the grain boundaries. Similarly, EDS results show a large presence of calcium and oxygen in the composite, with significant amounts of silicon, iron, and carbon, while sparing amounts of magnesium is present in the sample. Results obtained show similar results with increasing calcium content and improved mechanical properties.

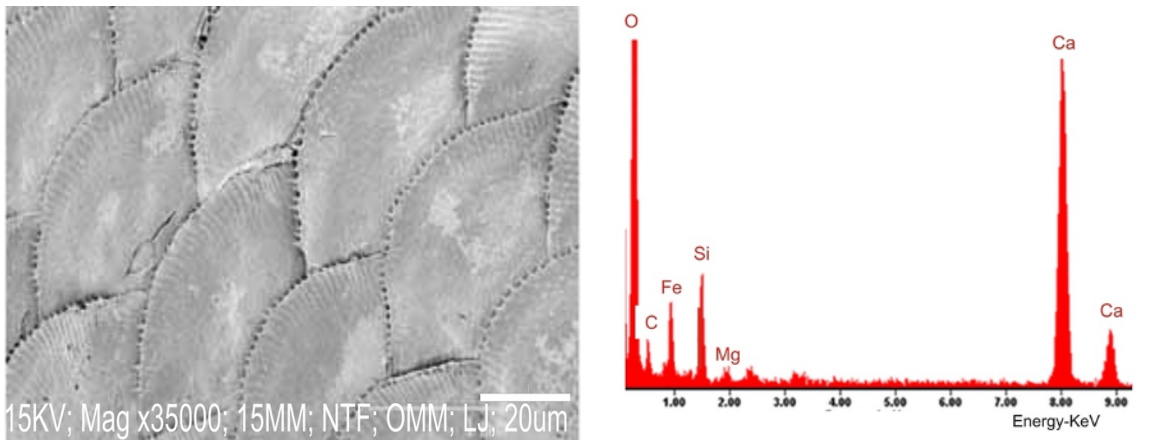


**Figure 4.6: (a) SEM image of AA6061 + 6 wt. % Chitosan. (b) EDS of specimen**

#### IV. SEM/EDS of reinforced AA6061 + 9 wt. % chitosan

The scanning electron micrograph (SEM) and energy dispersive spectroscopy (EDS) of the composite, AA6061 + 9 wt. % chitosan, is shown in Figure 4.7 a and b. The micrograph is obtained at a magnification of 35000X with an acceleration voltage of 15 kV and a working distance of 20 μm. From the SEM, it is observed that uniform distribution of chitosan particles in the aluminium alloy (AA6061) base matrix occurred during fabrication. This is evident in the micrograph as the structure of the composite show chitosan particulates reinforced into the grain boundaries of the AA6061 alloy matrix for support. However, a fracture is observed in the micrograph. The fracture is a result of handling after the stirring was done. Furthermore, jagged boundaries containing reinforcements are observed as opposed to the 3 wt. % chitosan sample with well-defined grain boundaries. Thus, the reinforcement is responsible for providing support to the continuous alloy matrix; ergo, the material has improved tensile strength compared to unreinforced alloy.

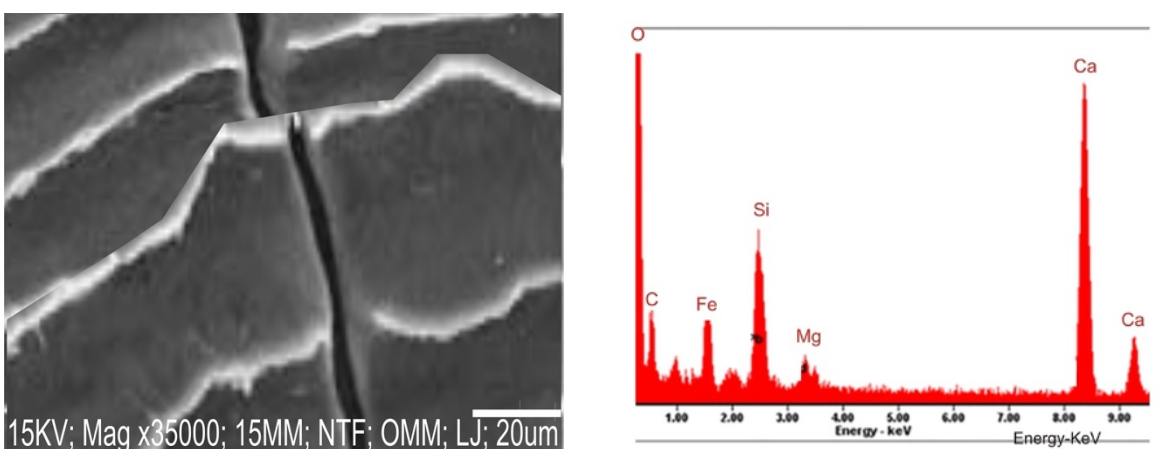


**Figure 4.7: (a) SEM image of AA6061 + 9 wt. % Chitosan. (b) EDS of specimen**

## V. SEM/EDS of specimen AA6061 + 12 wt.% chitosan

Figure 4.8 a and b shows the scanning electron micrograph (SEM) and energy dispersive spectroscopy (EDS) of the composite AA6061 + 12 wt. % chitosan obtained at magnification 33000 and a working distance of 100micro meters. High chitosan content is thoroughly dispersed in the alloy matrix fusing together the alloy grains. However, there appears to be an excessive amount of chitosan in the deficient AA6061 grain boundary, which is responsible for the observable roughness and appearance of pores in the surface morphology. There is no sign of cracks in the cast metal matrix composite. The EDS shows peaks of calcium, oxygen, essential elements in the hydroxyapatite ( $\text{Ca}_{10}(\text{PO}_4)_6(\text{OH})_2$ ), which is contained in the chitosan particles.

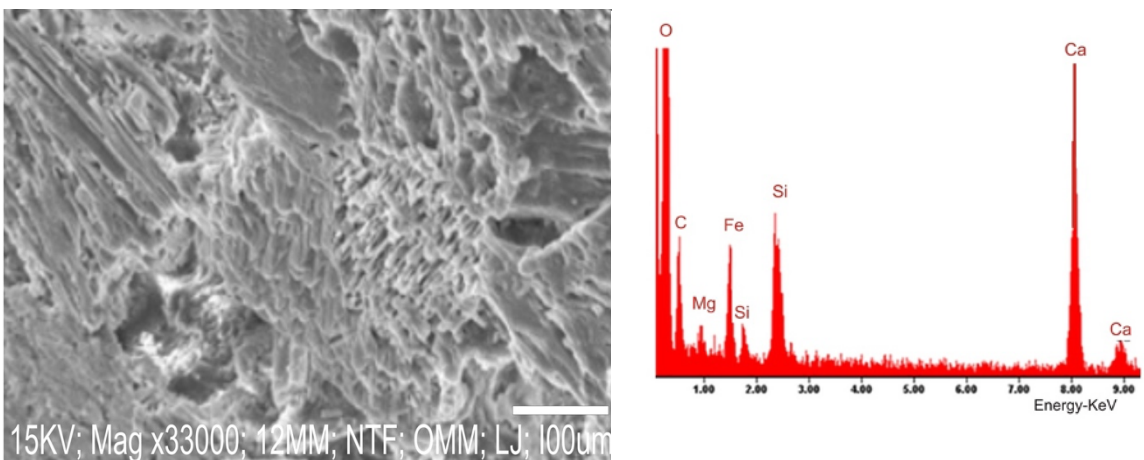


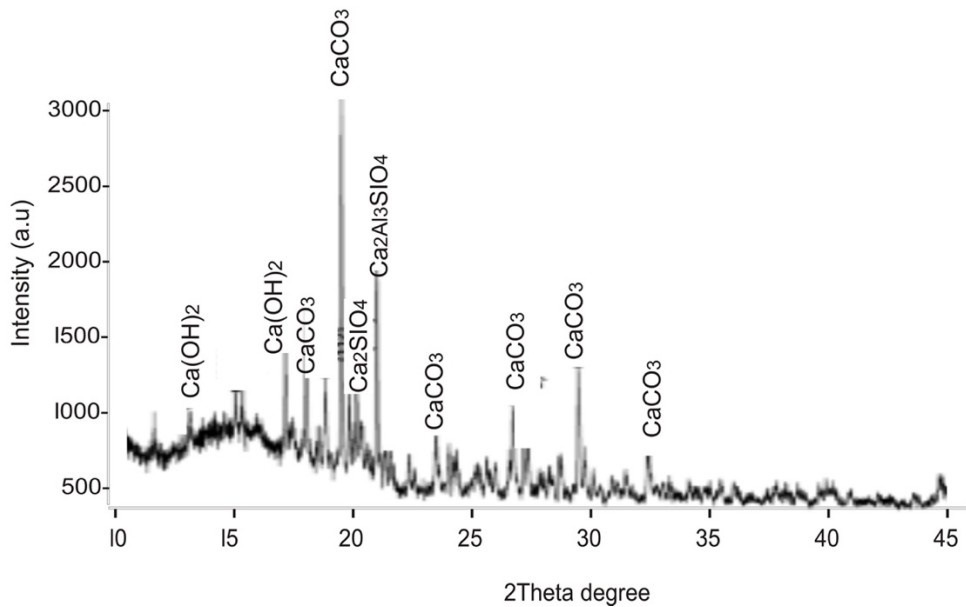
**Figure 4.8: (a) SEM image of AA6061 + 12 wt. % Chitosan. (b) EDS of specimen**

The micrograph images were obtained at configurations: 30000X, 33000X, and 35000X magnification with an acceleration voltage of 15 kV and a working distance between 20 and 100  $\mu\text{m}$ . Furthermore, from the images, an agglomeration of chitosan reinforcement particles was observed homogenously distributed in the region of the alloy's matrix. This composite exhibits improved mechanical properties compared to the unreinforced alloy. The Energy Disperse Spectroscopy images show the constituent elements of the AA6061 + 12 wt. % chitosan sample. The peaks of the constituent elements are observed to be calcium, oxygen, silicon, iron, carbon peaks, which are also the primary constituents of the reinforcements being considered.

#### 4.2.4 X-ray diffraction analysis of reinforced composites

X-ray diffraction analysis was performed on the unreinforced aluminium alloy (AA6061), and the sample was obtained from reinforcing AA6061 with chitosan at varying mass fractions of reinforcements. The analysis is done to identify the crystal structure of the materials. A Rigaku D/Max-111C was used to perform this analysis. The diffraction data (d value and relative intensity) obtained using Bragg's law was compared to the current powder diffraction file developed by the ICDD (International Center for Diffraction Data) containing 1,047,661 unique materials. Similar diffraction data means the same minerals to standard minerals that exist in the sample

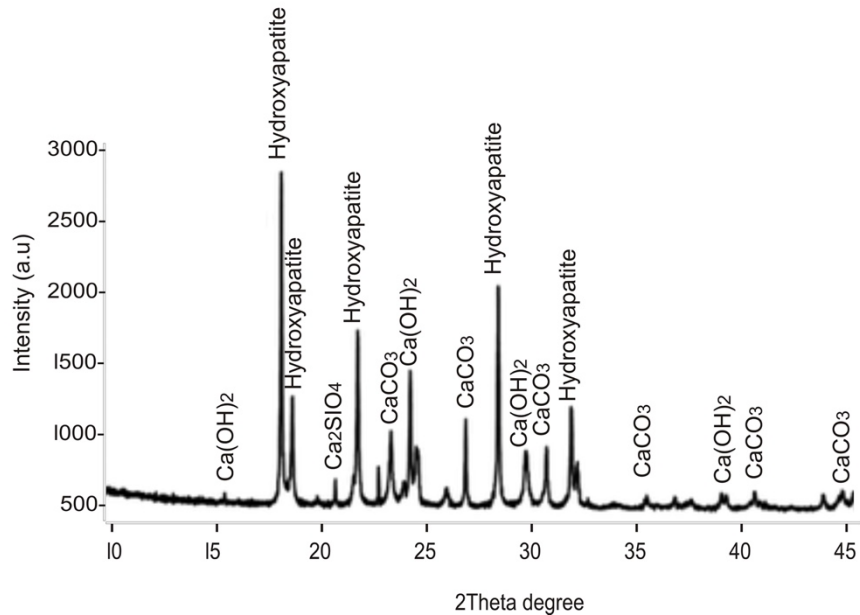
In Figure 4.9, the XRD analysis of the unreinforced alloy AA6061 is represented. The intensity counts to 3000 against Bragg's angle,  $2\theta$ , between 10 degrees and 45 degrees. The distinct hill-slope pattern in the diffractogram shows the presence of amorphous material within the alloy mixture. Furthermore, multiple instances occurrence of  $\text{CaCO}_3$ ,  $\text{Ca}_2\text{Al}_3\text{SiO}_4$ , and  $\text{Ca}(\text{OH})_2$  solidifies evidence of the presence of those compounds in the crystalline compound. With the  $\text{CaCO}_3$  crystalline phase having an intensity of 3000. In the  $\text{Ca}_2\text{Al}_3\text{SiO}_4$  crystalline phase, the material was indeed developed from aluminium alloy AA6061.



**Figure 4.9: XRD Spectrum of pure As-received Aluminium Alloy**

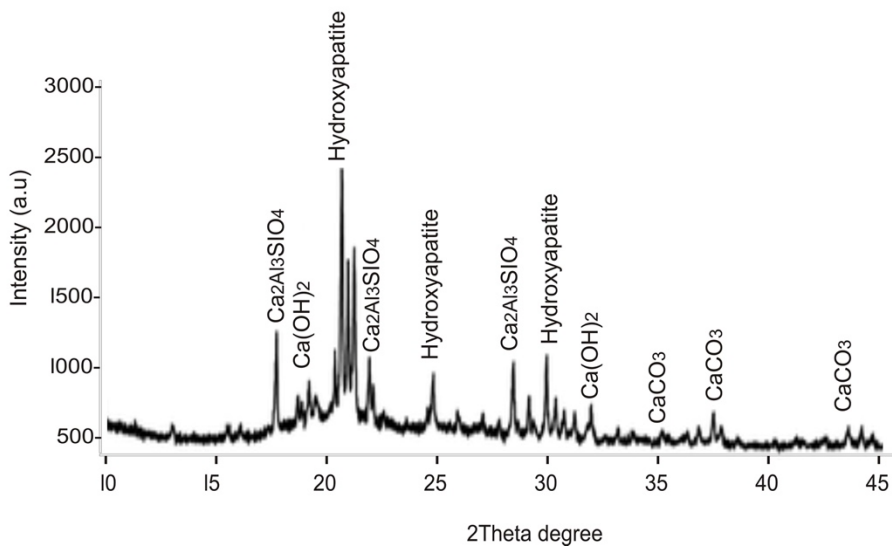
In Figure 4.10, the XRD analysis of the unreinforced alloy AA6061 is represented. The intensity counts up to 3000 against Bragg's angle,  $2\theta$ , between 10 degrees and 45 degrees. The peak intensities are observed for crystals of Hydroxyapatite  $\text{CaCO}_3$  and  $\text{Ca}(\text{OH})_2$ , respectively.

Furthermore, the diffractogram shows multiple peak instances of the crystalline phase: hydroxyapatite,  $\text{CaCO}_3$  and  $\text{Ca}(\text{OH})_2$  solidifying evidence of their presence in the composite. Likewise, a low hill-like slope between 10 and 15  $2\theta$  angle shows the small presence of amorphous composite in the composite mixture. The XRD pattern obtained proves the existence of particulate reinforcement materials used in this study, with hydroxyapatite being a constituent crystal of bone and teeth for strength and rigidity. Finally, XRD analysis of 3 wt. % chitosan reinforcement in AA6061 shows an increase in the number of phases compared to the pure alloy.



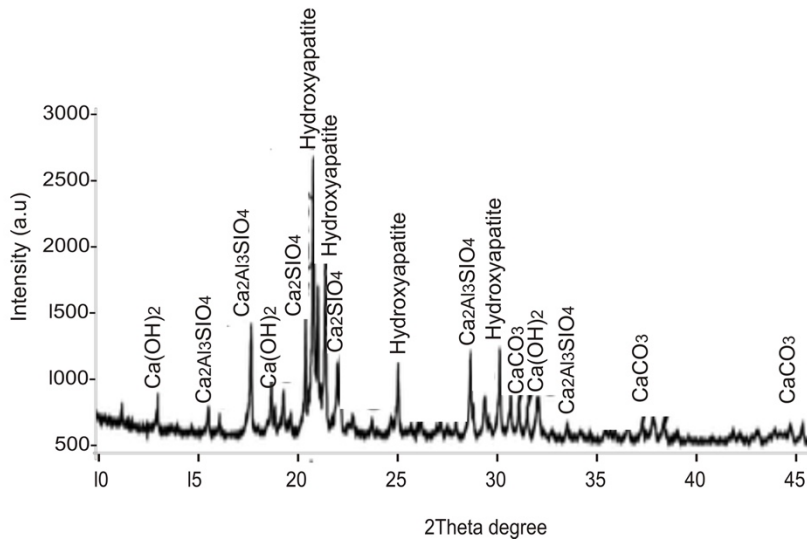
**Figure 4.10: XRD of AA6061 + 3 wt. % chitosan**

Figure 4.11 shows the X-ray Diffractogram analysis of the AA6061+ 6 wt. % chitosan. The diagram shows crystals diffracted between Bragg's angle,  $2\theta$ , of 10 degrees and 45 degrees. Furthermore, the peak phases in the analysis were hydroxyapatite,  $\text{Ca}_2\text{Al}_3\text{SiO}_4$ ,  $\text{CaCO}_3$ , and  $\text{Ca}(\text{OH})_2$ . respectively. The analysis shows multiple peaks of the crystalline phase: hydroxyapatite,  $\text{Ca}_2\text{Al}_3\text{SiO}_4$ ,  $\text{CaCO}_3$ , and  $\text{Ca}(\text{OH})_2$ . The XRD pattern obtained proves the existence of particulate reinforcement materials used in this study, with hydroxyapatite being a constituent crystal of bone and teeth for strength and rigidity. This XRD pattern obtained proves the existence of particulate in the composite. Also, it is observed that the composite containing 6 wt. % chitosan has a lower intensity reading than that of the fabricated sample with 3 wt. % chitosan.



**Figure 4.11: XRD of AA6061 + 6 wt. % chitosan**

In Figure 4.12, the XRD analysis of the AA6061 + 9 wt. % chitosan. The intensity counts up to 3000 against Bragg's angle,  $2\theta$ , between 10 degrees and 45 degrees with maximum intensity recorded slightly above 2500. Furthermore, the peak phases in the analysis are hydroxyapatite,  $\text{Ca}_2\text{Al}_3\text{SiO}_4$ ,  $\text{CaCO}_3$ , and  $\text{Ca}(\text{OH})_2$ . respectively. The analysis shows multiple peaks of the crystalline phase: hydroxyapatite,  $\text{Ca}_2\text{Al}_3\text{SiO}_4$ ,  $\text{CaCO}_3$ , and  $\text{Ca}(\text{OH})_2$ . This XRD pattern obtained proves the existence of these particulates in the composite.



**Figure 4.12: XRD of AA6061 + 9 wt. % chitosan**

Quantitative Analysis of crystalline constituent of AA6061+ 12 wt. % chitosan is represented in Figure 4.13 as diffractogram of intensity (a.u) against Bragg's angle,  $2\theta$ , between 10 degrees and 45 degrees. The diffractogram shows multiple crystalline constituents of the sample, with

peak intensity above 2500 in the phase hydroxyapatite. The peak phases in the analysis were hydroxyapatite,  $\text{Ca}_2\text{Al}_3\text{SiO}_4$ ,  $\text{CaCO}_3$ , and  $\text{Ca}(\text{OH})_2$ . respectively. The biogenic crystal, hydroxyapatite, is evidence of chitosan obtained from fish scales as reinforcement in the material.

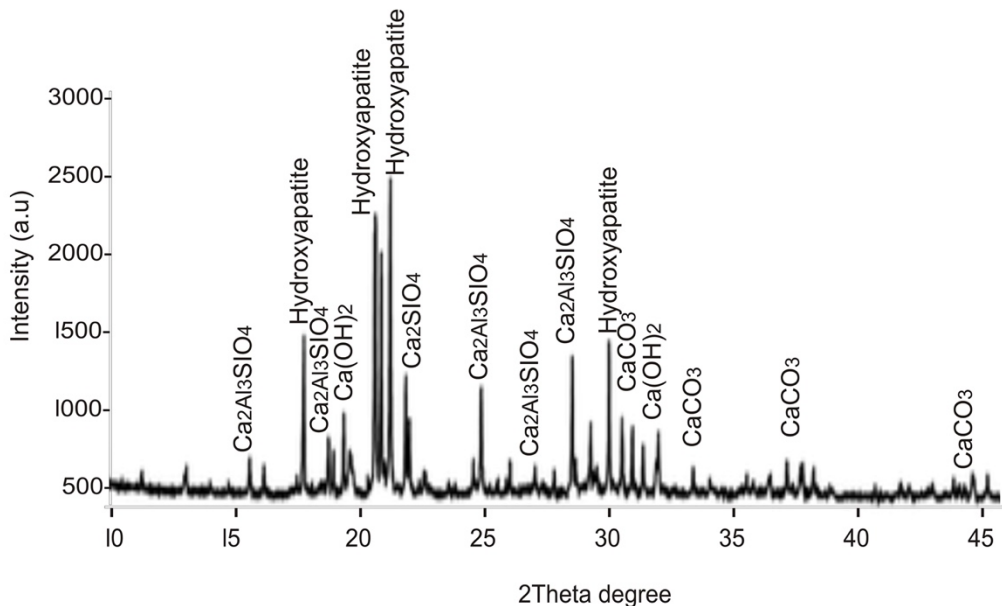


**Figure 4.13: XRD of AA6061 + 12 wt. % chitosan**

AA6061 reinforced with kaolinite chitosan composites for all weight percentages of (0, 3, 6, 9, 12) wt. % were investigated to detect the occurrence of reinforcement particles as well as the occurrence of unwanted materials. The patterns of diffraction were recorded to confirm the presence of kaolin chitosan in the composite. The sample is in powder form so that it can be easily placed in a sample holder of dimension 24.6 mm x 1.0 mm. the test was conducted. The XRD shows the peaks and phases of potential combinations of aluminium and chitosan particles. The figures above show that the main crystal phases present are Hydroxyapatite,  $\text{Ca}_2\text{Al}_3\text{SiO}_4$ ,  $\text{CaCO}_3$ , and  $\text{Ca}(\text{OH})_2$ , which are the highest, second highest and third highest peaks, respectively. The peaks were identified by following the JCPDC manual.

#### 4.2.5 Thermal properties: conductive heat transfer coefficient

The heat transfer coefficient is an important thermal property in the selection of materials for industrial use. In Figure 4.16, the conductive heat transfer coefficient is represented for unreinforced alloy and each of the developed composites. The calculated mean heat transfer coefficient for the composites reinforced with 3, 6, 9 and 12 wt. % chitosan increased with the increasing weight proportions from 124.16 to 189.40 W/m°C, as seen in Table 4.6. However, the addition of chitosan failed to improve the overall thermal conductivity of the unreinforced alloy AA6061, which was obtained as 362.97 W/m°C. Thus, while the reinforcement reduced the thermal contact resistance between grains in the alloy matrix, its composition of silicon, calcium, and oxygen which are majorly poor thermal conductor with low thermal conductivity resulted in an overall thermal conductivity decrease.

Similarly, results obtained from the addition of graphite-silicon carbide to aluminium alloy show lower thermal conductivity with added hybrid reinforcement of high silicon content compared to that of the as-cast alloy (Krishna et al., 2016). Therefore, the reinforcement resulted in increased density of alloy matrix structure, limiting the flow of electrons. The results obtain still show high thermal conductivity for the AA6061- chitosan composite, which is suitable for electronic packaging requiring heat management such as fins for microprocessor units in computers.

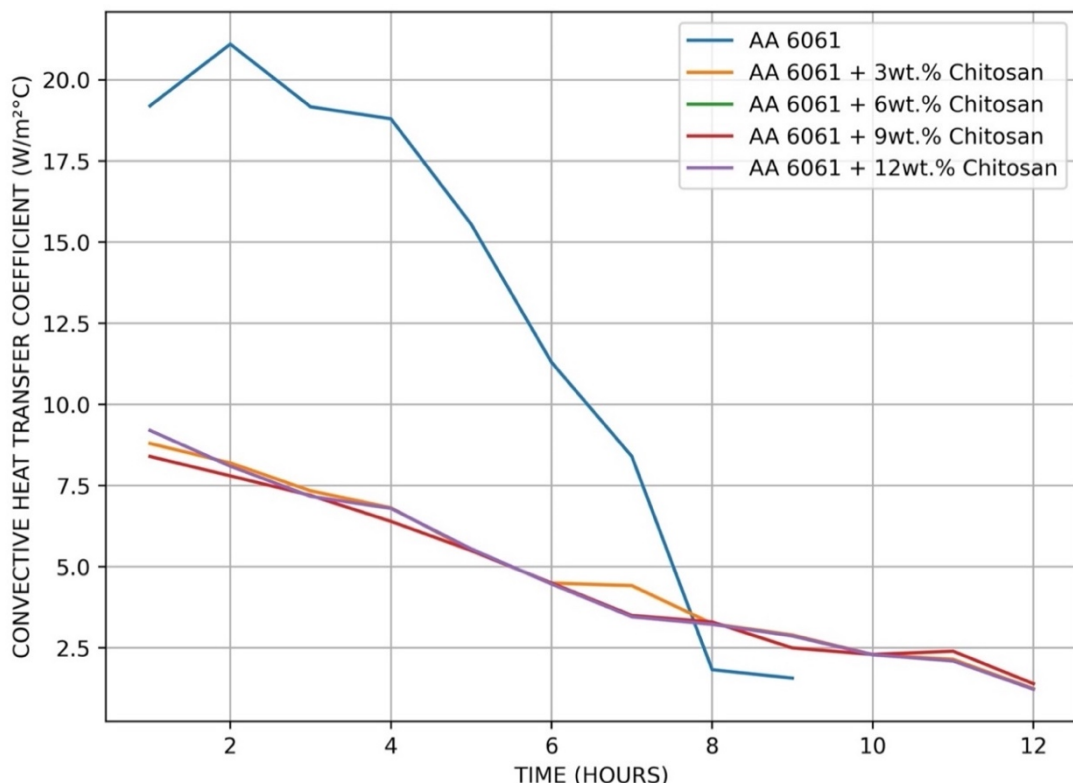
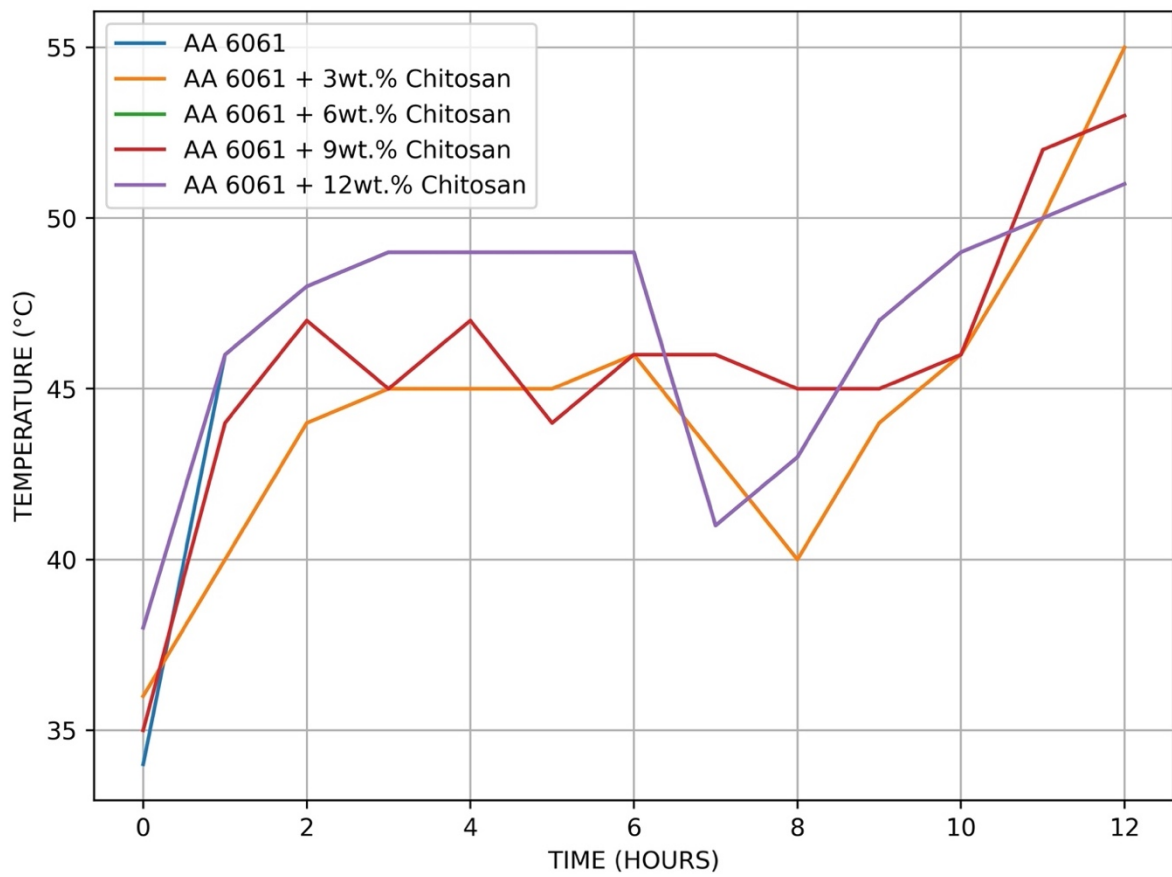
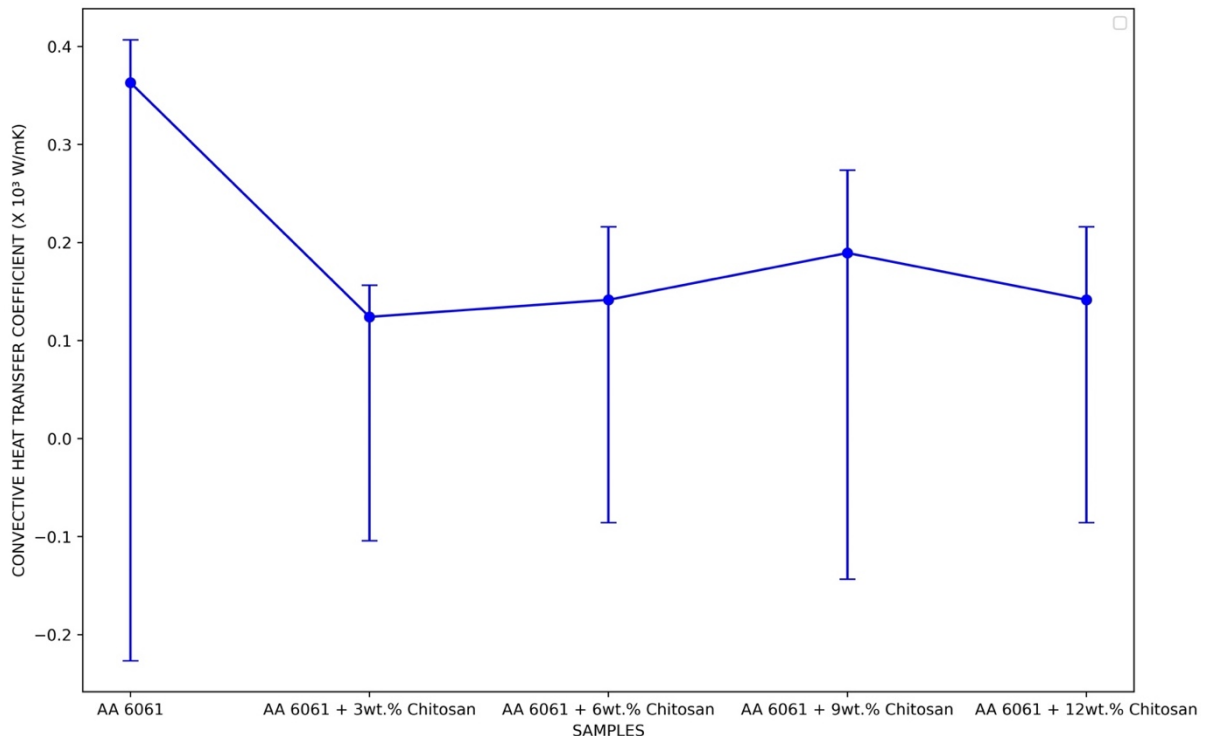


Figure 4.14: Surface Convective Heat Transfer Coefficient



**Figure 4.15: Surface Temperature of Composite**



**Figure 4.16: Error bars of Conductive Heat Transfer Coefficient of Samples.**

**Table 4.7: Result of Heat Transfer Coefficient of Composite.**

Specimen	Conductive Heat Transfer Coefficient (W/mK)
AA 6061	362.97
AA 6061 + 3 wt. % Chitosan	124.16
AA 6061 + 6 wt. % Chitosan	141.59
AA 6061 + 9 wt. % Chitosan	189.40
AA 6061 + 12 wt. % Chitosan	141.59

#### 4.2.6 Electrical properties: resistivity and conductivity

The conductivity of aluminium varies considerably between 30S/m and 65 S/m, depending upon the metal's chemical composition and physical properties (The Aluminium Association, 2015; Wang et al., 2021). Figure 4.17 and Figure 4.18 conductivity represent the samples' electrical properties, conductivity, and resistivity. Linear regression analysis is utilized in computing the values from the current values obtained in the experiment. In the analysis, conductance and resistance for unreinforced aluminium alloy, AA 6061, was determined to be 37.81 S/m and 0.026 Ωm, respectively. However, the analysis established a non-linear relationship between the introduction of chitosan into the AA6061 matrix.

Furthermore, substantial improvement in Conductivity of the unreinforced alloy was observed on the 12 wt. % chitosan composite. The sample had a conductivity of 38.197186 S/m, a marginal improvement of 1.035 % in the electrical property of AA6061. However, there is an observable trend of increase in conductivity from 3 wt. % to 12 wt. % of chitosan. Conversely, the resistivity of the fabricated samples diminished with an increase in the weight proportions of reinforcement. Thus, further research should be done on reinforcements above 12 wt. % for greater conductivity improvements.

**Table 4.8: Result of Electrical Resistivity and Conductivity of Samples**

Specimen	Maximum Voltage (V)	Maximum Current (A)	Resistance ( $\Omega$ )	Resistivity ( $\Omega\text{m}$ )	Conductivity (S/m)
AA 6061	0.5	1.19	0.421	0.026	37.81
AA 6061 + 3wt.% Chitosan	0.5	1.14	0.440	0.028	36.21
AA 6061 + 6wt.% Chitosan	0.5	1.15	0.435	0.027	36.61
AA 6061 + 9wt.% Chitosan	0.5	1.12	0.448	0.028	35.49
AA 6061 + 12wt.% Chitosan	0.5	1.20	0.417	0.026	38.20

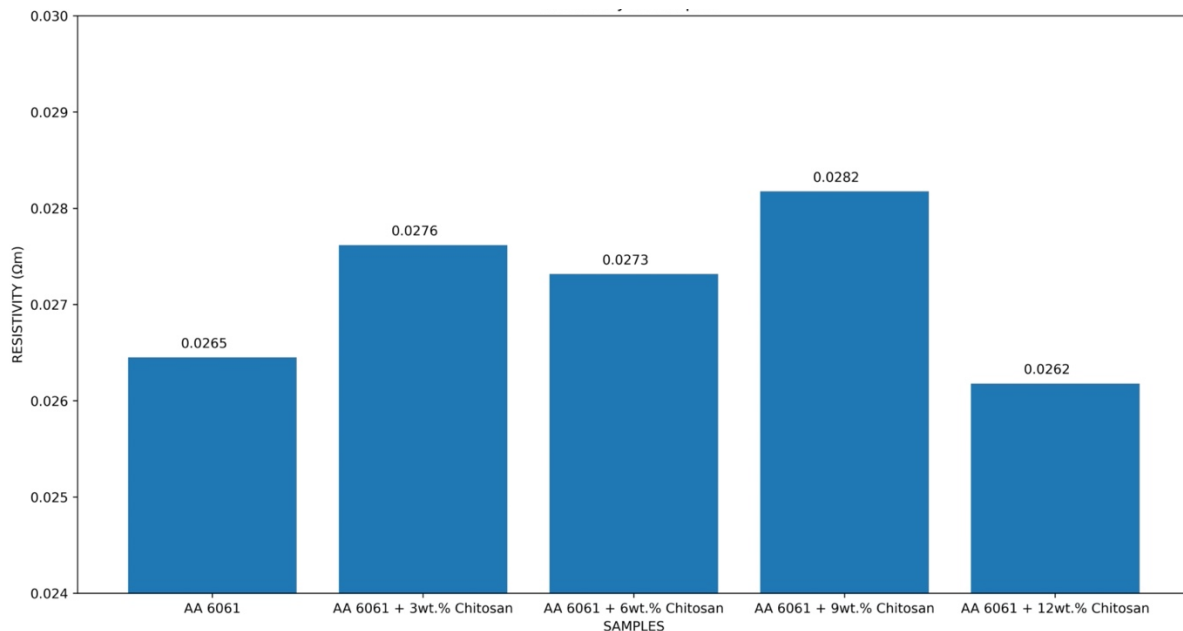


**Figure 4.17: Effects of Chitosan on Resistivity of AA6061**

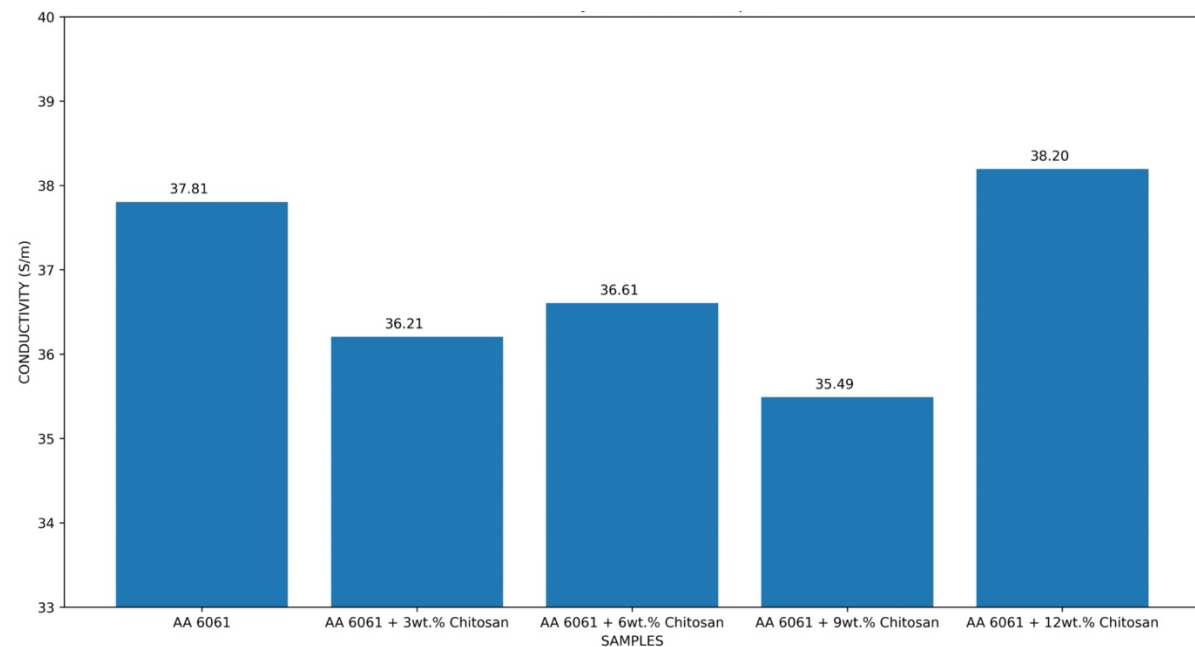


**Figure 4.18: Effects of Chitosan on Conductivity of AA6061**

## CHAPTER FIVE

### 5 CONCLUSION AND RECOMMENDATIONS

#### 5.1 Introduction

The drive towards protecting the earth has led material scientists towards exploring new sustainable materials, especially composites. However, these materials would not be incorporated into industries if the materials are not economical to fabricate and satisfy certain mechanical, thermal, electrical, and morphological requirements. This study provides a comprehensive assessment of chitosan as an agro-waste reinforcement and direction for exploring other composite reinforcements for aluminium alloy (AA6061).

#### 5.2 Conclusion

This research project developed the aluminium metal matrix composite (AMMC) by consolidating the AA6061 bulk matrix with chitosan at varying mass fractions. Furthermore, the mechanical, electrical, morphological, crystallographic, and thermal properties of the composites are analysed. An evaluation of results obtained compared to that of unreinforced alloy implied an increase in the weight proportion of reinforcement in the aluminium alloy matrix caused improvement in the material properties. The following have been discovered from this research project;

- Fish-scales-derived chitosan particles of  $90 \mu\text{m}$  can serve as reinforcement of AA6061 alloy in the fabrication of AMMCs.
- Surface Morphology of composites improved with the addition of chitosan, with the most defined structure attained at the addition of 9 wt. % chitosan.
- Brinell's hardness test showed an increase in value with an increase in mass fraction of chitosan.
- The tensile strength improved significantly with increasing weight fraction of reinforcement and attained up to 25.8 % improvement with 12 wt. % chitosan.
- Electrical and thermal conductivity rose marginally with increasing chitosan reinforcement peaking at  $39.172 \text{ S/m}$ , which is  $0.391 \text{ S/m}$  greater than that of the unreinforced alloy.

### **5.3 Final Conclusion**

This study utilises agricultural waste in developing a novel material and presents a novel material. Thus, it promotes metallurgist, material, and design engineers' attention to the environment in selecting materials for use. The results were derived to show the feasibility of applying the fabricated composite in the manufacturing of electronic devices as a heat sink for thermal management as well as low weight electrical cooking appliances such as electric cookers. Furthermore, improved mechanical strength properties signify the value of applying developed composite in engine development as a material for piston fabrication.

### **5.4 Recommendations**

From the results, my recommendations are as follows.

- Further investigation should be conducted on the developed samples to understand their fatigue, wear, and response surface analysis.
- Investigation on effects of stir casting parameters on composite could be used to develop modified stir casting technique to avoid agglomeration further and ensure uniform distribution of reinforcement.
- Also, the two-step stir casting techniques were used for fabrication. Improved stir-casting or other liquid (in-situ) fabrication methods should be applied.
- Additional studies should be carried out using various chitosan weight fractions for specific properties, significantly above 12 wt. % chitosan for mechanical (tensile and hardness), electrical and thermal properties.
- Experiments should be carried out on the inclusion of another reinforcement to form a hybrid composite.

## REFERENCES

- Abba, H. A., Nur, I. Z., & Salit, S. M. (2013). Review of Agro Waste Plastic Composites Production. *Journal of Minerals and Materials Characterization and Engineering*, 2013, 271–279.
- Adekunle, A. S., Adeleke, A. A., Ikubanni, P. P., Omoniyi, P. O., Gbadamosi, T. A., & Odusote, J. K. (2020). Effect of copper addition and solution heat treatment on the mechanical properties of aluminum alloy using formulated bio-quenchant oils. *Engineering and Applied Science Research*, 47(3), 297–305.
- Adeodu, A., Mudashiru, L., Daniyan, I., & Awodoyin, A. (2020). Effect of silver nanoparticle (AgNp) mixed with calcium carbonate on impact, hardness and tensile strength properties of aluminium 6063. *Journal of Composite Materials*.
- Ahmed, S., & Ikram, S. (2017). Chitosan: Derivatives, Composites and Applications. In *Scrivener Publishing*.
- Aigbodion, V. S., Ozor, P. O., Eke, M. N., & Nwoji, C. U. (2021). Explicit microstructure, corrosion, and stress analysis of value-added Al-3.7%Cu-1.4%Mg/1.5% rice husk ash nanoparticles for pump impeller application. *Chemical Data Collections*, 33, 100675.
- Alaneme, K. K., Okotete, E. A., Fajemisin, A. V., & Bodunrin, M. O. (2019). Applicability of metallic reinforcements for mechanical performance enhancement in metal matrix composites: a review. *Arab Journal of Basic and Applied Sciences*, 26(1), 311–330.
- Alaneme, K. K., & Sanusi, K. O. (2015). Microstructural characteristics, mechanical and wear behaviour of aluminium matrix hybrid composites reinforced with alumina, rice husk ash and graphite. *Engineering Science and Technology, an International Journal*, 18(3), 416–422.
- Aribo, S., Fakorede, A., Ige, O., & Olubambi, P. (2017). Erosion-corrosion behaviour of aluminum alloy 6063 hybrid composite. *Wear*, 376–377, 608–614.
- Arora, G., & Sharma, S. (2018). A Comparative Study of AA6351 Mono-Composites Reinforced with Synthetic and Agro Waste Reinforcement. *International Journal of Precision Engineering and Manufacturing*, 19(4), 631–638.
- Atuanya, C. U., Ibhadode, A. O. A., & Dagwa, I. M. (2012). Effects of breadfruit seed hull ash on the microstructures and properties of Al-Si-Fe alloy/breadfruit seed hull ash particulate composites. *Results in Physics*, 2, 142–149.
- Atuanya, C. U., Onukwuli, O. D., & Aigbodion, V. S. (2014). Experimental correlation of wear parameters in Al-Si-Fe alloy/breadfruit seed hull ash particulate composites. *Journal of*

- Composite Materials*, 48(12), 1487–1496.
- Bannaravuri, P. K., & Birru, A. K. (2018). Strengthening of mechanical and tribological properties of Al-4.5%Cu matrix alloy with the addition of bamboo leaf ash. *Results in Physics*, 10, 360–373.
- Bhaskar, S., Kumar, M., & Patnaik, A. (2020). Silicon Carbide Ceramic Particulate Reinforced AA2024 Alloy Composite - Part I: Evaluation of Mechanical and Sliding Tribology Performance. *Silicon*, 12(4), 843–865.
- Bisaria, H., Gupta, M. K., Shandilya, P., & Srivastava, R. K. (2015). Effect of Fibre Length on Mechanical Properties of Randomly Oriented Short Jute Fibre Reinforced Epoxy Composite. *Materials Today: Proceedings*, 2(4–5), 1193–1199.
- Bodunrin, M. O., Alaneme, K. K., & Chown, L. H. (2015). Aluminium matrix hybrid composites: A review of reinforcement philosophies; Mechanical, corrosion and tribological characteristics. *Journal of Materials Research and Technology*, 4(4), 434–445.
- Carlsson, L. A., Adams, D. F., & Pipes, R. B. (2014). Experimental Characterization of Advanced Composite Materials. In *Experimental Characterization of Advanced Composite Materials*, (4 th ed.). CRC Press.
- Carron, J., Weber, L., Molina, J., & Rhe, M. (2008). *Thermal conductivity of aluminum matrix composites reinforced with mixtures of diamond and SiC particles*. 58, 393–396.
- Chawla, K. K. (2012). Composite materials: Science and engineering, third edition. In *Composite Materials: Science and Engineering, Third Edition* (Issue 1994).
- Chawla, K. K. (2016). Composite materials: Science and engineering. Springer.
- Chen, C. L., & Lin, C. H. (2017). A study on the aging behavior of al6061 composites reinforced with Y<sub>2</sub>O<sub>3</sub> and TiC. *Metals*, 7(1).
- Chen, P., Fan, X., Yang, Q., Zhang, Z., Jia, Z., & Liu, Q. (2021). Creep behavior and microstructural evolution of 8030 aluminum alloys compressed at intermediate temperature. *Journal of Materials Research and Technology*, 12, 1755–1761. <https://doi.org/10.1016/j.jmrt.2021.07.012>
- Chu, K., Jia, C., Liang, X., Chen, H., Gao, W., & Guo, H. (2009). Modeling the thermal conductivity of diamond reinforced aluminium matrix composites with inhomogeneous interfacial conductance. *Materials and Design*, 30(10), 4311–4316.
- Crini, G., & Hatchett, C. (2019). Historical review on chitin and chitosan biopolymers. *Environmental Chemistry Letters*, Ilkewitsch 1908.
- Daramola, O. O., Adediran, A. A., & Fadumiye, A. T. (2015). Evaluation of the mechanical

- properties and corrosion behaviour of coconut shell ash reinforced aluminium (6063) alloy composites. *Leonardo Electronic Journal of Practices and Technologies*, 14(27).
- David Raja Selvam, J., Dinaharan, I., Vibin Philip, S., & Mashinini, P. M. (2018). Microstructure and mechanical characterization of in situ synthesized AA6061/(TiB<sub>2</sub>+Al<sub>2</sub>O<sub>3</sub>) hybrid aluminum matrix composites. *Journal of Alloys and Compounds*, 740, 529–535.
- Davis, J. R. (2001). Aluminum and Aluminum Alloys Introduction and Overview. *ASM International*, 351–416.
- Dwivedi, S. P., Maurya, M., Maurya, N. K., Srivastava, A. K., Sharma, S., & Saxena, A. (2020). Utilization of groundnut shell as reinforcement in development of aluminum based composite to reduce environment pollution: A review. *Evergreen*, 7(1), 15–25.
- Dwivedi, S. P., Sharma, S., & Mishra, R. K. (2016). Synthesis and mechanical behaviour of green metal matrix composites using waste eggshells as reinforcement material. *Green Processing and Synthesis*, 5(3), 275–282.
- Emara, M. M. (2017). Enhanced tensile, hardness and wear behaviors of pure aluminum matrix reinforced with steel chips via powder metallurgy technique. *IOP Conference Series: Materials Science and Engineering*, 191(1), 12041.
- Ermolaeva, N. S., Kaveline, K. G., & Spoormaker, J. L. (2002). Materials selection combined with optimal structural design: Concept and some results. In *Materials and Design*, 23(5).
- Ertugrul, O., He, T., Shahid, R. N., & Scudino, S. (2019). Effect of heat treatment on microstructure and mechanical properties of Al 2024 matrix composites reinforced with Ni60Nb40 metallic glass particles. *Journal of Alloys and Compounds*, 808, 151732.
- Fayomi OSI, Akande IG, Atayero AAA et al. (2019) Electro-mechanical, microstructure and corrosion properties of 85Al6063-15CFBP alloy for advance applications. *Journal of Materials and Environmental Sciences*, 10(11), 1152–1161
- Georgantzia, E., Gkantou, M., & Kamaris, G. S. (2021). Aluminium alloys as structural material: A review of research. *Engineering Structures*, 227, 111372.
- Ghanaraja, S., Vinuth Kumar, K. L., Raju, H. P., & Ravikumar, K. S. (2015). Processing and Mechanical Properties of Hot Extruded Al (Mg)-Al<sub>2</sub>O<sub>3</sub> Composites. *Materials Today: Proceedings*, 2(4–5), 1291–1300.
- Ghanbari, D., Kasiri Asgarani, M., Amini, K., & Gharavi, F. (2017a). Influence of heat treatment on mechanical properties and microstructure of the Al2024/SiC composite produced by multi-pass friction stir processing. *Measurement: Journal of the*

- International Measurement Confederation*, 104, 151–158.
- Ghanbari, D., Kasiri Asgarani, M., Amini, K., & Gharavi, F. (2017b). Influence of heat treatment on mechanical properties and microstructure of the Al2024/SiC composite produced by multi-pass friction stir processing. *Measurement: Journal of the International Measurement Confederation*, 104, 151–158.
- Gladston, J. A. K., Dinaharan, I., Sheriff, N. M., & Selvam, J. D. R. (2017). Dry sliding wear behavior of AA6061 aluminum alloy composites reinforced rice husk ash particulates produced using compocasting. *Journal of Asian Ceramic Societies*, 5(2), 127–135.
- Gokulalakshmi, E., Ramalingam, K., Umasankari, & Vanitha, M. (2017). Extraction and Characterization of Chitosan Obtained from Scales of Clarias gariepinus (Catfish). *Biotechnology Journal International*, 18(4), 1–8.
- Gopalakrishnan, S., & Murugan, N. (2012). Production and wear characterisation of AA 6061 matrix titanium carbide particulate reinforced composite by enhanced stir casting method. *Composites Part B: Engineering*, 43(2), 302–308.
- Hatchett C (1799) Experiments and observations on shell and bone. In *Bowyer W, Nichols J (eds) Philos Trans R Soc Lond. Royal Society*, London, 89(18), 315–334
- Hima Gireesh, C., Durga Prasad, K. G., Ramji, K., & Vinay, P. V. (2018). Mechanical Characterization of Aluminium Metal Matrix Composite Reinforced with Aloe vera powder. *Materials Today: Proceedings*, 5(2), 3289–3297.
- Jacob, S., Shajin, S., & Gnanavel, C. (2017). Thermal analysis on Al7075/Al<sub>2</sub>O<sub>3</sub> metal matrix composites fabricated by stir casting process. *IOP Conference Series: Materials Science and Engineering*, 183(1).
- Jayalakshmi, S., Singh, A., & Gupta, M. (2016). Synthesis of Light Metal Nanocomposites: Challenges and Opportunities. *Indian Journal of Advances in Chemical Science, October*, 283–288.
- Jayashree, P. ., Shankar, M. . G., Achutha, K., Sharma, S. ., & Raviraj, S. (2013). Review on Effect of Silicon Carbide (SiC) on Stir Cast Aluminium Metal Matrix Hybrid Composites. *International Journal of Current Engineering and Technology*, 766–767, 293–300.
- Joseph, O. O., & Babaremu, K. O. (2019). Agricultural waste as a reinforcement particulate for aluminum metal matrix composite (AMMCs): A review. *Fibers*, 7(4).
- Kalel, S. M., & Patil, S. R. (2018). Ceramic Reinforced Metal Matrix Composite ( MMC ) - Processing. *International Journal of Advance Research in Science and Engineering, Mmc*, 1047–1058.

- Kareem, A., Qudeiri, J. A., Abdudeen, A., Ahammed, T., & Ziout, A. (2021). A review on aa 6061 metal matrix composites produced by stir casting. *Materials*, 14(1), 1–22.
- Khan, A., Khan, R. A., Salmieri, S., Le Tien, C., Riedl, B., Bouchard, J., Chauve, G., Tan, V., Kamal, M. R., & Lacroix, M. (2012). Mechanical and barrier properties of nanocrystalline cellulose reinforced chitosan based nanocomposite films. *Carbohydrate Polymers*, 90(4), 1601–1608.
- Krishna, S. A. M., Shridhar, T. N., & Krishnamurthy, L. (2016). Microstructural characterization and investigation of thermal conductivity behaviour of Al 6061-SiC-Gr hybrid metal matrix composites. *Indian Journal of Engineering and Materials Sciences*, 23(4), 207–222.
- Kulkarni P., P., Siddeswarappa B., Shivashankar, K., & Hemanth Kumar, K. S. (2019). A Survey on Effect of Agro Waste Ash as Reinforcement on Aluminium Base Metal Matrix Composites. *Open Journal of Composite Materials*, 9, 312–326.
- Kumar, A., & Tiwari, G. N. (2007). Effect of mass on convective mass transfer coefficient during open sun and greenhouse drying of onion flakes. *Journal of Food Engineering*, 79(4), 1337–1350.
- Kumar, B. P., & Birru, A. K. (2017). Microstructure and mechanical properties of aluminium metal matrix composites with addition of bamboo leaf ash by stir casting method. *Transactions of Nonferrous Metals Society of China (English Edition)*, 27(12), 2555–2572.
- Kumar, D. (2021). Morphological and Mechanical Characterization of Al-4032 / SiC / GMP Hybrid Composites. 1–15.
- Kumar, R. A., Devaraju, A., & Arunkumar, S. (2018). Experimental Investigation on Mechanical Behaviour and Wear Parameters of TiC and Graphite Reinforced Aluminium Hybrid Composites. *Materials Today: Proceedings*, 5(6), 14244–14251.
- Kumar, S., Singh, R., & Hashmi, M. S. J. (2020). Metal matrix composite: a methodological review. *Advances in Materials and Processing Technologies*, 6(1), 13–24.
- Kumar, V. M., & Venkatesh, C. V. (2019). A comprehensive review on material selection, processing, characterization and applications of aluminium metal matrix composites. *Materials Research Express*, 6(7), 072001.
- Kurzawa, A., Pyka, D., Jamroziak, K., Bocian, M., Kotowski, P., & Widomski, P. (2018). Analysis of ballistic resistance of composites based on EN AC-44200 aluminum alloy reinforced with Al<sub>2</sub>O<sub>3</sub> particles. *Composite Structures*, 201(2017), 834–844.

- Li, X., Yan, H., Wang, Z. W., Li, N., Liu, J. L., & Nie, Q. (2019). Effect of heat treatment on the microstructure and mechanical properties of a composite made of Al-Si-Cu-Mg aluminum alloy reinforced with sic particles. *Metals*, 9(11), 1–9.
- Li, Z., & Gao, W. (2008). Oxidation of metal matrix composites. In *Developments in High-Temperature Corrosion and Protection of Materials*, Elsevier Ltd, 365–397.
- Liu, S., Wang, Y., Muthuramalingam, T., & Anbucheziyan, G. (2019). Effect of B4C and MoS<sub>2</sub> reinforcement on micro structure and wear properties of aluminum hybrid composite for automotive applications. *Composites Part B: Engineering*, 176, 107329.
- Ma, M., Lai, R., Qin, J., Wang, B., Liu, H., & Yi, D. (2021). Effect of weld reinforcement on tensile and fatigue properties of 5083 aluminum metal inert gas (MIG) welded joint: Experiments and numerical simulations. *International Journal of Fatigue*, 144.
- Mahesh Kumar, V., & Venkatesh, C. V. (2018). Effect of ceramic reinforcement on mechanical properties of aluminum matrix composites produced by stir casting process. *Materials Today: Proceedings*, 5(1), 2466–2473.
- Manda, C. S., Babu, B. S., & Ramaniah, N. (2021). Effect of Heat Treatment on Mechanical properties of Aluminium metal matrix composite (AA6061/MoS<sub>2</sub>). *Advances in Materials and Processing Technologies*, 1–18.
- Mehta, V. R., & Sutaria, M. P. (2020). Investigation on the Effect of Stirring Process Parameters on the Dispersion of SiC Particles Inside Melting Crucible. *Metals and Materials International*, 27(8), 2989-3002.
- Miller, W. S., Zhuang, L., Bottema, J., Wittebrood, A. J., De Smet, P., Haszler, A., & Vieregge, A. (2000). Recent development in aluminium alloys for the automotive industry. *Materials Science and Engineering A*, 280(1), 37–49.
- Mohanavel, V., Suresh Kumar, S., Sathish, T., Adithiyaa, T., & Mariyappan, K. (2018). Microstructure and mechanical properties of hard ceramic particulate reinforced AA7075 alloy composites via liquid metallurgy route. *Materials Today: Proceedings*, 5(13), 26860–26865.
- Nayim, S. M. T. I., Hasan, M. Z., Seth, P. P., Gupta, P., Thakur, S., Kumar, D., & Jamwal, A. (2020). Effect of CNT and TiC hybrid reinforcement on the micro-mechano-tribo behaviour of aluminium matrix composites. *Materials Today: Proceedings*, 21, 1421–1424.
- Neto de Oliveira Sousa, V., & Nascimento, R. F. (2017). Recent progress in biocomposite of biodegradable polymer. In *Handbook of Composites from Renewable Materials* (Vols. 1–

- 8, Issue December 2020).
- Nyanor, P., El-Kady, O., Yehia, H. M., Hamada, A. S., Nakamura, K., & Hassan, M. A. (2021). Effect of Carbon Nanotube (CNT) Content on the Hardness, Wear Resistance and Thermal Expansion of In-Situ Reduced Graphene Oxide (rGO)-Reinforced Aluminum Matrix Composites. *Metals and Materials International*, 27(5), 1315–1326.
- Ogawa, F., Yamamoto, S., & Masuda, C. (2018). Strong, ductile, and thermally conductive carbon nanotube-reinforced aluminum matrix composites fabricated by ball-milling and hot extrusion of powders encapsulated in aluminum containers. *Materials Science and Engineering A*, 711(2017), 460–469.
- Omoniyi, P., Adekunle, A., Ibitoye, S., Olorunpomi, O., & Abolusoro, O. (2021). Mechanical and microstructural evaluation of aluminium matrix composite reinforced with wood particles. *Journal of King Saud University - Engineering Sciences*.
- Orhadahwe, T. A., Ajide, O. O., Adeleke, A. A., & Ikubanni, P. P. (2020). A review on primary synthesis and secondary treatment of aluminium matrix composites. *Arab Journal of Basic and Applied Sciences*, 27(1), 389–405.
- Patience, G. S. (2013). Physicochemical Analysis. In *Experimental Methods and Instrumentation for Chemical Engineers*.
- Pawar, P., Wabale, R., & Utpat, A. (2018). A comprehensive study of aluminum based metal matrix composites: Challenges and opportunities. *Materials Today: Proceedings*, 5(11), 23937-23944.
- Porwal, H., Grasso, S., & Reece, M. J. (2013). Review of graphene–ceramic matrix composites. *Advances in Applied Ceramics*, 112(8), 443-454.
- Praveen, P., & Yarlagadda, P. K. D. V. (2005). Meeting challenges in welding of aluminum alloys through pulse gas metal arc welding. *Journal of Materials Processing Technology*, 164–165, 1106–1112.
- Reddy, M. P., Himyan, M. A., Ubaid, F., Shakoor, R. A., Vyasaraj, M., Gururaj, P., Yusuf, M., Mohamed, A. M. A., & Gupta, M. (2018). Enhancing thermal and mechanical response of aluminum using nanolength scale TiC ceramic reinforcement. *Ceramics International*, 44(8), 9247–9254.
- Roebben, G., Steen, M., Bressers, J., & Van der Biest, O. (1996). Mechanical fatigue in monolithic non-transforming ceramics. *Progress in Materials Science*, 40(4), 265-331.
- Roy, U., & Roy, P. K. (2020). Advances in heat intensification techniques in shell and tube heat exchanger. In *Advanced Analytic and Control Techniques for Thermal Systems with*

- Heat Exchangers*. Elsevier Inc.
- Sanusi, K. O., Akinlabi, E. T., Muzenda, E., & Akinlabi, S. A. (2015). Enhancement of Corrosion Resistance Behaviour of Frictional Stir Spot Welding of Copper. *Materials Today: Proceedings*, 2(4–5), 1157–1165.
- Saravanan, S. D., & Kumar, M. S. (2013). Effect of mechanical properties on rice husk ash reinforced aluminum alloy (AlSi10Mg) matrix composites. *Procedia Engineering*, 64, 1505–1513.
- Sathish, T., Saravanan, S., & Vijayan, V. (2020). Effect of reinforced aluminium alloy LM30 with pure ceramic particles to evaluate hardness and wear properties. *Materials Research Innovations*, 24(3), 129–132.
- Satish Kumar, T., Shalini, S., & Krishna Kumar, K. (2020). Effect of friction stir processing and hybrid reinforcement on wear behaviour of AA6082 alloy composite. *Materials Research Express*, 7(2).
- Schier J. F., & Juergens R. J. (1983). Astronautics and Aeronautics, 44.
- Sekaran Raja, P., Ganesh Kumar, S., Anix Joel Singh, J., & Vairamuthu, J. (2020). Experiment investigation and analysis of fish scale reinforced polymer composite materials. *Materials Today: Proceedings*, 33, 4542-4545.
- Shankar, S., Balaji, A., & Kawin, N. (2018). Investigations on mechanical and tribological properties of Al-Si10-Mg alloy/sugarcane bagasse ash particulate composites. *Particulate Science and Technology*, 36(6), 762–770.
- Shankar, S., & Elango, S. (2017). Dry Sliding Wear Behavior of Palmyra Shell Ash-Reinforced Aluminum Matrix (AlSi10Mg) Composites. *Tribology Transactions*, 60(3), 469–478.
- Sharma, A. K., Bhandari, R., Aherwar, A., & Pinca-Bretorean, C. (2020). A study of fabrication methods of aluminum based composites focused on stir casting process. *Materials Today: Proceedings*, 27, 1608–1612.
- Shirvanimoghaddam, K., Khayyam, H., Abdizadeh, H., Karbalaei Akbari, M., Pakseresht, A. H., Ghasali, E., & Naebe, M. (2016). Boron carbide reinforced aluminium matrix composite: Physical, mechanical characterization and mathematical modelling. *Materials Science and Engineering A*, 658, 135–149.
- Shrivastava, V., Gupta, G. K., & Singh, I. B. (2019). Heat treatment effect on the microstructure and corrosion behavior of Al-6061 alloy with influence of  $\alpha$ -nanoalumina reinforcement in 3.5% NaCl solution. *Journal of Alloys and Compounds*, 775, 628–638.

- Sijo, M. T., & Jayadevan, K. R. (2016). Analysis of Stir Cast Aluminium Silicon Carbide Metal Matrix Composite: A Comprehensive Review. *Procedia Technology*, 24, 379–385.
- Singh, B. (2018). Rice husk ash. In *Waste and Supplementary Cementitious Materials in Concrete: Characterisation, Properties and Applications*. Elsevier Ltd.
- Sivakumar, S., Golla, B. R., & Rajulapati, K. V. (2019). Influence of ZrB<sub>2</sub> hard ceramic reinforcement on mechanical and wear properties of aluminum. *Ceramics International*, 45(6), 7055–7070.
- Smith, W. F., Hashemi, J., & Presuel-Moreno, F. (2019). *Foundations of Materials Science and Engineering Sixth Edition*.
- Soundhar, A., & Jayakrishna, K. (2019). Investigations on mechanical and morphological characterization of chitosan reinforced polymer nanocomposites. *Materials Research Express*, 6(7).
- Stalin, B., Sudha, G. T., Kailasanathan, C., & Ravichandran, M. (2020). Effect of MoO<sub>3</sub> ceramic oxide reinforcement particulates on the microstructure and corrosion behaviour of Al alloy composites processed by P/M route. *Materials Today Communications*, 25, 101655.
- The Aluminium Association. (2015). International Alloy Designations and Chemical Composition Limits for Wrought Aluminum and Wrought Aluminum Alloys With Support for On-line Access From: Aluminum Extruders Council Use of the Information. *The Aluminum Association, Arlington, Virginia, Enero 2015*, 31.
- Tiwari, S., & Pradhan, M. K. (2017). Effect of rice husk ash on properties of aluminium alloys: A review. *Materials Today: Proceedings*, 4(2), 486–495.
- Udoye, N. E., Inegbenebor, A. O., & Fayomi, O. S. I. (2019). The Study on Improvement of Aluminium Alloy for Engineering Application: A Review. *International Journal of Mechanical Engineering and Technology (IJMET)*, 10(3), 380–385.
- Umanath, K., Selvamani, S. T., Palanikumar, K. K., & Niranjanavarma, D. (2014). Metal to metal worn surface of AA6061 hybrid composites casted by stir casting method. *Procedia Engineering*, 97, 703–712.
- Wang, Y., Zhu, L., Niu, G., & Mao, J. (2021). Conductive Al Alloys: The Contradiction between Strength and Electrical Conductivity. *Advanced Engineering Materials*, 23(5), 1–22.
- Waterman, N. A. (1982). Computer aided materials selection. *Materials and Design*, 3(4), 502–503.

- Yadav, A. K., Pandey, K. M., & Dey, A. (2018). Aluminium Metal Matrix Composite with Rice Husk as Reinforcement: A Review. *Materials Today: Proceedings*, 5(9), 20130–20137.
- Yogeshwaran, S., Natrayan, L., Rajaraman, S., Parthasarathi, S., & Nestro, S. (2020). Experimental investigation on mechanical properties of Epoxy/graphene/fish scale and fermented spinach hybrid bio composite by hand lay-up technique. *Materials Today: Proceedings*, 37(2), 1578–1583.
- Zakaria, H. M. (2014). Microstructural and corrosion behavior of Al/SiC metal matrix composites. *Ain Shams Engineering Journal*, 5(3), 831–838.
- Zeller, D., Cashion, T., Palomares, M., & Pauly, D. (2018). Global marine fisheries discards: A synthesis of reconstructed data. *Fish and Fisheries*, 19(1), 30–39.